INVESTIGATING THE HETEROGENEITY OF GLUCOSE AND GLUTAMINE METABOLISM IN CANCER

A Dissertation

Presented to the Faculty of the Graduate School

of Cornell University

In Partial Fulfillment of the Requirements for the Degree of

Doctor of Philosophy

by

Ahmad Abdul Rahman Cluntun

August 2017

INVESTIGATING THE HETEROGENIETY OF GLUCOSE AND GLUTAMINE METABOLISM IN CANCER

Ahmad Abdul Rahman Cluntun, Ph.D.

Cornell University 2017

Rapidly proliferating cancer cells have increased biosynthetic and bioenergetic needs compared to quiescent cells. Hence, they undergo a reprogramming of intermediary metabolism, mainly by upregulating the uptake and catabolism of certain nutrients. The classical example of this is the 'Warburg effect' or aerobic glycolysis, defined as an increase in glucose uptake coupled to lactate secretion, regardless of oxygen availability in cancer cells. One consequence of this is that the majority of glucose carbon is diverted away from the mitochondria and the tricarboxylic acid (TCA) cycle, and secreted out of the cell as lactate. This prompts some cancer cells to exhibit an increased dependence on glutamine metabolism to refill the TCA cycle. However, recent studies have uncovered widespread heterogeneity on the roles of glucose and glutamine metabolism in cancer cells, prompting a need for further clarification.

In order to examine these metabolic pathways in cancer cells, I first helped develop high-resolution LC-MS metabolomic workflows. The initial objective of my thesis focused on the Warburg effect, and specifically, the increased rate of glycolytic flux that occurs in colon cancer cells. I demonstrated that changes in glycolytic flux could modify specific histone acylation marks in a dose-dependent manner, suggesting that a possible function of the Warburg effect is to confer specific signaling effects on cancer cells.

The second objective of my thesis focused on defining the contribution of the mitochondrial glutaminase isoenzyme GLS2 on the observed variability in glutamine

dependence in various breast cancer cell types. I identified GLS2 as an important metabolically active enzyme in breast cancer cells that can feed TCA cycle anaplerosis. This finding has important clinical implications due to the fact that a glutaminase inhibitor, which fails to block GLS2 activity, is currently in Phase II trials.

In summary, my dissertation work further contributes to our fundamental understanding of the metabolic programs operating in cancer cells, by uncovering novel aspects of both glucose and glutamine metabolism. This work identifies new underlying causes of the metabolic heterogeneity observed in cancer cells and may prove relevant to future improvements in cancer therapies.

BIOGRAPHICAL SKETCH

The author was born in the ancient holy city of Makkah, located in the western region of the Kingdom of Saudi Arabia. Soon thereafter his father earned the opportunity to pursue his graduate studies in the United States of America where the family would live for eight years. The family would move again to the Kingdom of Bahrain and live there for another six years before returning to Saudi Arabia. The author pursued undergrad studies at King Saud University, where he majored in clinical laboratory sciences. Upon graduation he worked at the molecular genetics core facility laboratory at the King Faisal Specialist Hospital and Research Center for two years as a medical technologist. Mirroring his father's career he then received a full scholarship to pursue a Masters degree in biochemistry and molecular biology from Georgetown University, where he met his wife Najla Al-Sweel. There he had the opportunity to work with Sona Vasudevan, who introduced him to the world of computational biology and bioinformatics. Both he and his wife then decided to pursue their Ph.D. graduate work at Cornell University. The author then joined Jason Locasale's laboratory as one of his first graduate students. There he helped develop high-resolution LC-MS metabolomic workflows to study cancer metabolism. His son Fouzan was born soon after passing his candidacy exam. He later joined Rick Cerione's lab after Jason relocated his lab to Duke University. There he switched his focus from glucose metabolism and histone acetylation to glutamine metabolism in cancer cells. The author looks forward to publishing the rest of his thesis work and pursuing a postdoctoral position. He aims to ultimately utilize all his education, training and network of collaborators to start his own lab back in Saudi Arabia.

To my mom Hafsa Qadah

Acknowledgments

This work would not have been possible without the generous financial support from the King Abdullah International Medical Research Center (KAIMRC).

Science is an apprenticeship and a collaborative endeavor, and ultimately you are only as good as your mentors and collaborators are. In that sense, I have been immensely fortunate and privileged to train under incredible mentors and work with outstanding collaborators during my Ph.D. tenure here at Cornell. Having had a unique Ph.D. experience, which included switching research groups, I could not have been able to get through it all without the help and support of many individuals.

I would like to express my sincere gratitude to my advisor Dr. Richard Cerione. He accepted me in to his research group, when my previous lab relocated, with open arms. He gave me the time, freedom and support to develop a new project. He addressed any of my needs or concerns whenever they emerged. I feel incredibly fortunate to have had the pleasure to be part of his lab, as I was able to witness what true leadership entails. Thank you for everything Rick.

I would also like to thank the various members of the Cerione lab, past and present. Namely, Dr. Jon Erickson, who, over the past couple of years, has served as my therapist, mentor and guru giving me sound advice and guidance both for my personal life and for my research project. Dr. Sekar Ramachandran for all of the great scientific discussions that would inspire me whenever I hit a roadblock. I could not have completed the writing of this thesis without their help and support, Thank you Ram and Jon.

I also have much gratitude to Dr. Michael Lukey for collaborating with me on the GLS2

project, and for inspiring me to be a better writer and a more careful investigator. Dr. Shawn Milano who was the first person I met when I joined the Cerione lab and went out of his way to make sure I instantly fit in and felt at home. Dr. Clint Stalnecker who collaborated with me on a few projects when I was in the Locasale lab and introduced me the Cerione lab. And to all the other great members of the Cerione lab, you all helped me in innumerate ways and I will always cherish your friendships and be inspired by your brilliance.

I would also like to thank Dr. Jason Locasale for his mentorship, support and guidance. He gave me priceless insights on what it takes to start a successful lab, and I will be forever grateful for the training I received in his lab. I would also like to thank the members of the Locasale lab, especially Dr. Xiaojing Liu, Sam, Mahya and Maria. Ultimately, I learned how to do science in this lab.

I would also like to thank my third committee member Dr. Hening Lin for always having an open door for me whenever I needed him and for all his support and insightful suggestions for my project.

I would also like to thank my collaborators from the University of Chicago, Dr. Yingming Zhao and Dr. He Huang who worked with me on the histone acylation project. I would also like to thank Dr. Patrick Stover and Olga for permitting me continued access to the LC-MS instrument.

I would also like to thank the many Cornell faculty members that helped sculpt my scientific thinking, specifically, Dr. Andy Clark and Dr. John Lis. I would also like to thank Dr. Volker Vogt, who I met two years prior to applying to Cornell and was one of the main reasons I decided to come here. He has been one of my biggest advocates and supporters and for that I will be forever grateful and indebted to him.

I would also like to thank the BMCB GFAs Vic, Casey, Ginger and Diane. You gals always knew what to say to brighten my day. I would also like to thank the many friends I made over the years here at Cornell, whether through the Cornell Saudi Club, MECA or BMCB. Your friendships will always be the greatest gift I obtained from Cornell.

I would like to thank my parents, Abdulrahman Cluntun and Hafsa Qadah, and my siblings, Ahlam, Ameera, Amjad, Abrar, Areej, Arwa, Rayan and Rashid, for their constant encouragement, support and love. The demands of earning a Ph.D. have kept me away from you, sometimes for multiple years at a time, forcing me to miss many birthdays, anniversaries, weddings and funerals. I am grateful to you for your understanding and forgiveness of my absence and for being the constant force that has allowed me to plow through all my difficulties.

Finally and most importantly, I would like to thank my wife, Najla Al-Sweel. Her support, encouragement, quiet patience and unwavering love were undeniably the bedrock upon which the past seven years of my life have been built on. Her tolerance of my occasional bad moods is a testament in itself of her unyielding devotion and love. How she managed to do all of that while getting through her own unique struggles as a Ph.D. student, as well as take care of both our son Fouzan and I, with such grace and excellence, never ceases to amaze me. Thank you Naj, we did it hun!

TABLE OF CONTENTS

LIST OF FIGURES

LIST OF TABLES

LIST OF ABBREVIATIONS

Gln: Glutamine

Glu: Glutamate

GSH: Glutathione

Asp: Aspartate

Ala: Alanine

Thr: Threonine

Gly: Glycine

Ser: Serine

Cys: Cysteine

Pro: Proline

Mal: Malate

Pyr: Pyruvate

Lac: Lactate

OAA: Oxaloacetate

Cit: Citrate

TCA: Tricarboxylic Acid (Citric acid) cycle

α-KG: alpha-ketoglutarate

Ac-CoA: acetyl-Coenzyme A

CoA: Coenzyme A

GBM: Glioblastoma

NSCLC: non-small cell lung carcinoma

PTMs: Posttranslational modifications

2DG: 2-Deoxy-D-Glucose

Veh: Vehicle

2DG6P: 2-deoxyglucose-6-phosphate

β-OHB: Beta-hydroxybutyrate

HDAC: Histone Deacetylase

KAT: Lysine acetyl transferases

Ac-H3: global acetylated histone H3

SILAC: Stable Isotopic Labeling by Amino acids in cell culture

K_{hib}: Lysine 2-hydroxyisobutyrylation

K_{bu}: Lysine Butyrylation

K_{pr}: Lysine Propionylation

K_{ac}: Lysine Acetylation

GLS: Glutaminase

GLS2: Glutaminase 2

PC: Pyruvate Carboxylase

GLUL: Glutamine Synthetase

MAT1A: S-adenosyl methionine synthetase

SAM: S-adenosyl methionine

IDH1: Isocitrate dehydrogenase 1

2-HG: 2-hydroxyglutarate

PDAC: Pancreatic ductal adenocarcinoma

LIST OF SYMBOLS

uM: microMolar

mM: milliMolar

M/Z: Mass over Charge ratio

um: micrometer

mm: millimeter

cm: centimeter

nL: nanoLiter

uL: microliter

mL: milliliter

U: Unit

v/v: volume/volume percent

w/w: weight/weight percent

ms: milliseconds

°C: degrees Celsius

ug: microgram

mg: milligram

N: Normal

kV: kiloVolts

ppm: parts per million

xg: times gravity

PREFACE

This dissertation is submitted for the degree of Doctor of Philosophy in the Field of Biochemistry, Molecular & Cell Biology at Cornell University. The research described in chapter two was conducted under the supervision of Dr. Jason W. Locasale in the Division if Nutritional Sciences at Cornell University, between July 2013 and August 2015. After his relocation to Duke University, I joined Professor Richard A. Cerione's research group. The research described in chapter three was conducted under his supervision in the Department of Chemistry and Chemical Biology at Cornell University, between August 2015 and August 2017. This work is to the best of my knowledge original, except where acknowledgements and references are made to previous work. Neither this, nor any substantially similar dissertation has been or is being submitted for any other degree, diploma of other qualification at any other university. This dissertation contains less than 30,000 words.

Part of this work has been presented in the following publications:

Lukey, M.J., **Cluntun, A.A.,** Katt, W.P., Druso, J.E., Lin, M.C. and Cerione, R.A., *Defining the roles of Glutaminase isozymes in breast cancer cells,* manuscript in preparation (co-first author)

Cluntun, A.A., Lukey, M.J, Cerione, R.A. and Locasale, J.W., *Glutamine metabolism in cancer: understanding the heterogeneity.* Trends in Cancer. 2017 **3**(3): p. 169-180.

Stalnecker C.A., **Cluntun, A.A.** and Cerione, R.A., *Balancing redox stress: anchorage-independent growth requires reductive carboxylation.* Translational Cancer Research, 2016. **5**(5): p. 504-511

Cluntun, A.A., Huang, H., Dai, L., Liu, X., Zhao, Y. and Locaslae, J.W., *The rate of glycolysis quantitatively mediates specific histone acetylation sites.* Cancer Metab, 2015. **3**: p. 10.

Shestov, A.A., Liu, X., Ser, Z., **Cluntun, A.A.**, Hung, Y.P., Huang, L., Kim, D., Le, A., Yellen, G., Albeck, J.G. and Locasale, J.W., *Quantitative determinants of aerobic glycolysis identify flux through the enzyme GAPDH as a limiting step.* Elife, 2014. **3**.

Liu, X., Ser, Z., **Cluntun, A.A.**, Mentch, S.J. and Locasale, J.W., *A strategy for sensitive, large scale quantitative metabolomics.* J Vis Exp, 2014(87).

Ahmad A. Cluntun

August 2017

Chapter 1

[*]Overview

Introduction

Cancer cells undergo a reprogramming of metabolism in order to maintain bioenergetics, redox status, cell signaling and biosynthesis, in what is often a poorly vascularized, nutrient-deprived microenvironment [1-4]. To supply biosynthetic pathways with precursors, the uptake and catabolism of certain nutrients are upregulated in tumor cells. For example, the 'Warburg effect', also known as aerobic glycolysis, is a phenomenon of increased glucose uptake coupled to lactate secretion, regardless of oxygen availability in cancer cells. This unique metabolic feature occurs in many human tumors, such that positron emission tomography (PET) using the glucose analog ^{18}F-flurodeoxyglucose is widely used for imaging tumors in the clinic [1, 5]. One consequence of the Warburg effect is that the majority of glucose carbon is diverted away from the mitochondria and the tricarboxylic acid (TCA) cycle, and secreted out of the cell as lactate, forcing the cell to find alternative sources to compensate for this. Correspondingly, many cancer cells display a dependence on an exogenous supply of glutamine; despite it being a non-essential amino acid (NEAA) that mammalian cells can synthesize *de novo* (Figure 1.1). However, beyond serving as a source of carbon to replenish the TCA cycle, glutamine also serves as an important source of reduced nitrogen for biosynthetic reactions, as well as a precursor to glutathione, nucleotides and lipid synthesis via reductive carboxylation (Figure 1.2) [1, 2, 6, 7]. Indeed, an inhibitor of the mitochondrial enzyme glutaminase, which converts glutamine to glutamate, a

[*] Adapted from Cluntun, A.A., et al. (2017) *Trends in Cancer.* **3**(3): p. 169-180.

Figure 1.1. The Warburg effect and TCA cycle anaplerosis.

The majority of glycolytic carbons are diverted away from the mitochondria and secreted as lactate. Glutamine metabolism can be utilized as an anaplerotic source of carbon to maintain the TCA cycle. Gln: Glutamine, Glu: Glutamate, α−KG: alpha-ketoglutatarate, TCA: Tricarboxylic acid cycle.

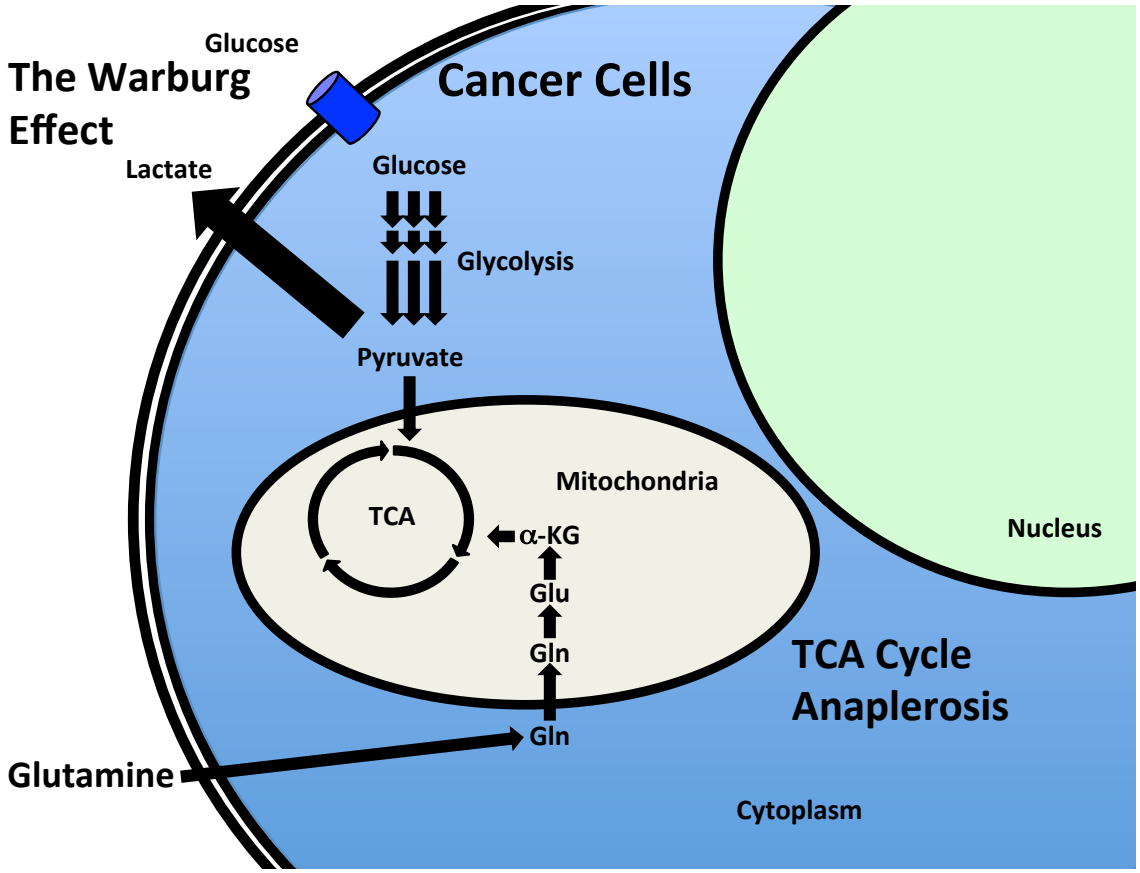
Glucose
The Warburg Effect
Cancer Cells
Lactate
Glucose
Glycolysis
Pyruvate
Mitochondria
TCA
α-KG
Glu
Gln
Gln
Nucleus
TCA Cycle Anaplerosis
Glutamine
Cytoplasm

precursor of the TCA cycle intermediate α-ketoglutarate (α-KG), is currently being evaluated in clinical trials for treatment of a range of malignancies [8-12]. Several recent studies have led to new insights in our understanding of the roles of both glucose and glutamine metabolism in cancer. For example, a recent study found that neither glucose nor glutamine is the source of the majority of cell mass in proliferating mammalian cells[13]. This was a counterintuitive finding as both glucose and glutamine have the highest consumption rates in these cells and yet non-glutamine amino acids, consumed at much slower rates, were determined to provide abundant carbon and nitrogen to these cells. Another important study revealed significant heterogeneity in glucose metabolism between patients and within individual lung tumors[14]. However, glutamine metabolism, in particular, has had a series of recent reports that has cast some doubt and confusion on its importance in cancer cells. In particular, a recent study found that the requirements for glutamine undergo changes upon transition from monolayer culture to anchorage-independent culture [7], and another study suggested that glutamine catabolism was not required for tumorigenesis *in vivo* in some mouse models, which led to the conclusion that glutamine metabolism may not have a role in cancer [15]. Nevertheless, numerous other studies have provided compelling evidence that a requirement for glutamine catabolism indeed exists in many *in vivo* settings [10, 16-23]. Here I will discuss these seemingly contradictory recent findings in detail and explain the factors underlying the heterogeneity of glutamine metabolism in cancer.

Figure 1.2. The glutamine metabolic footprint in cancer.

Glutamine has a five-carbon backbone and two nitrogen atoms (α and γ) to donate. Glutamine's metabolic footprint goes well beyond TCA cycle anaplerosis. Gln: Glutamine, Glu: Glutamate, GSH: Glutathione, Asp: Aspartate, Ala: Alanine, Thr: Threonine, Gly: Glycine, Ser: Serine, Cys: Cysteine, Pro: Proline, Mal: Malate, Pyr: Pyruvate, Lac: Lactate, OAA: Oxaloacetate, Cit: Citrate, TCA: Citric acid cycle, α-KG: alpha-ketoglutarate.

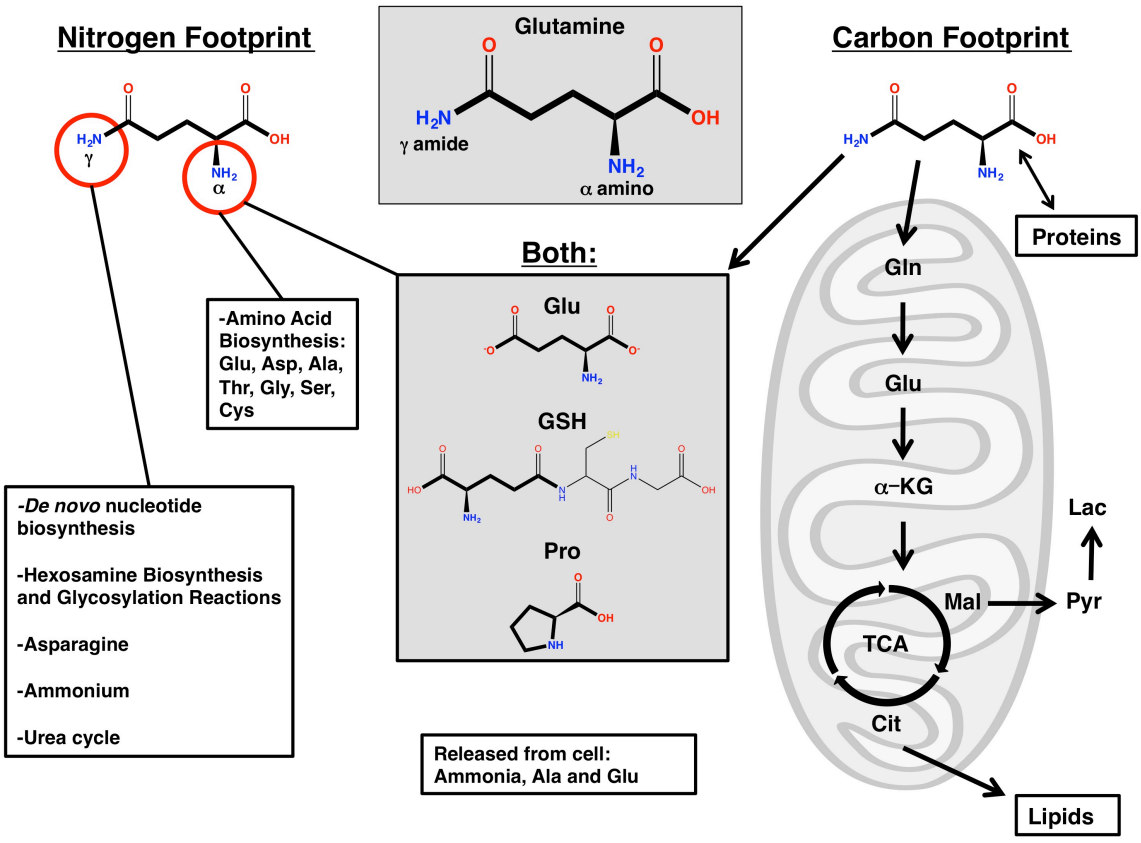
Nitrogen Footprint
Glutamine
γ amide
α amino
Carbon Footprint
Proteins
Both:
Glu
GSH
Pro
-Amino Acid Biosynthesis: Glu, Asp, Ala, Thr, Gly, Ser, Cys
-De novo nucleotide biosynthesis
-Hexosamine Biosynthesis and Glycosylation Reactions
-Asparagine
-Ammonium
-Urea cycle
Released from cell: Ammonia, Ala and Glu
Gln
Glu
α-KG
Lac
Mal
Pyr
TCA
Cit
Lipids

Culture conditions and model systems influence glutamine metabolism

The ability to culture cell lines derived from human tumors has, over the past 60 years, provided researchers with a powerful tool for studying cancer biology. A common characteristic of mammalian cell lines grown in culture, noted by Harry Eagle in the 1950s [24], is a dependence on an abundant exogenous supply of the NEAA glutamine. After glucose, glutamine is the most rapidly consumed nutrient by many human cancer cell lines grown in culture [13, 25]. However, glutamine requirements are very heterogeneous among different cancer cell lines, ranging from those that are glutamine auxotrophs, to those that can survive and proliferate in the absence of an exogenous glutamine supply [20, 26]. Recent studies have demonstrated that the tissue of origin, the underlying genetics, and the microenvironment, can all impact cancer cell metabolism, including utilization of glutamine. Importantly, tumor microenvironment conditions can be modeled ***ex vivo***, as the constituents of the culture media can be customized and other essential variables that determine metabolic requirements such as oxygen levels can be controlled [27, 28].

In monolayer culture, the non-small cell lung cancer (NSCLC) cell line H460 shows abundant uptake of glutamine, which is primarily utilized for TCA cycle anaplerosis. However, when the same cells are grown under anchorage-independent conditions as tumor spheroids, glutamine oxidation is suppressed and instead reductive glutamine metabolism *via* cytosolic isocitrate dehydrogenase 1 (IDH1) occurs [7]. The isocitrate/citrate generated by IDH1 then enters the mitochondria and undergoes oxidative metabolism *via* IDH2, generating mitochondrial NADPH to mitigate the elevated reactive oxygen species (ROS) levels that occur during anchorage-independent growth.

Distinct metabolic alterations take place when NSCLC cells are transitioned from an *ex*

vivo to an *in vivo* environment. When cells derived from mutant *KRAS*-driven NSCLC tumors are grown in culture, glutamine supplies the TCA cycle with carbon, and inhibition of the mitochondrial enzyme glutaminase (GLS) suppresses cell proliferation [15]. However, this glutamine-dependent phenotype is lost when the same cells are grown as lung tumors in mice. Instead, TCA cycle intermediates in the tumors are derived primarily from glucose *via* glycolysis and the enzyme pyruvate carboxylase (PC), and tumors are resistant to glutaminase inhibition or to CRISPR/Cas9-mediated *GLS* deletion [15]. At first glance, these findings may seem surprising and contradictory to previous reports regarding the importance of glutamine metabolism in cancer cells both *ex vivo* and *in vivo* (see Table 1). However, they are consistent with earlier studies showing that some NSCLC tumors in human patients rely on glucose-derived carbon and PC activity, and show upregulated *PC* gene expression [29]. Indeed, PC has been identified as an essential factor in cancer cells that display glutamine-independent growth [30]. Nevertheless, many tumors rely on glutamine-mediated TCA cycle anaplerosis *in vivo* with concordance of glutamine dependence *ex vivo* and *in vivo.* (see Table 1), as discussed in detail below [9, 10, 12, 16, 17, 31] (Figure 1.3). Thus, recent observations in certain NSCLC mouse tumors cannot be generalized to other cancers.

Figure 1.3. TCA cycle anaplerotic fluxes affect glutaminase inhibition efficacy.

There are two main anaplerotic fluxes that can feed the citric acid cycle, a glutamine flux via glutaminase (GLS and/or GLS2) and a glucose flux via pyruvate carboxylase (PC). Glutamine synthetase (GLUL) is also an important enzyme for this process as it can synthesize glutamine from glutamate and thus allow cells to survive in glutamine-depleted conditions. The expression levels of these enzymes vary according to tissue type and can greatly affect their sensitivity to glutaminase inhibition. GBM: Glioblastoma, NSCLC: non-small cell lung carcinoma, Pyr: Pyruvate, Lac: Lactate, Cit: Citrate, TCA: Citric acid cycle, α-KG: alpha-ketoglutarate.

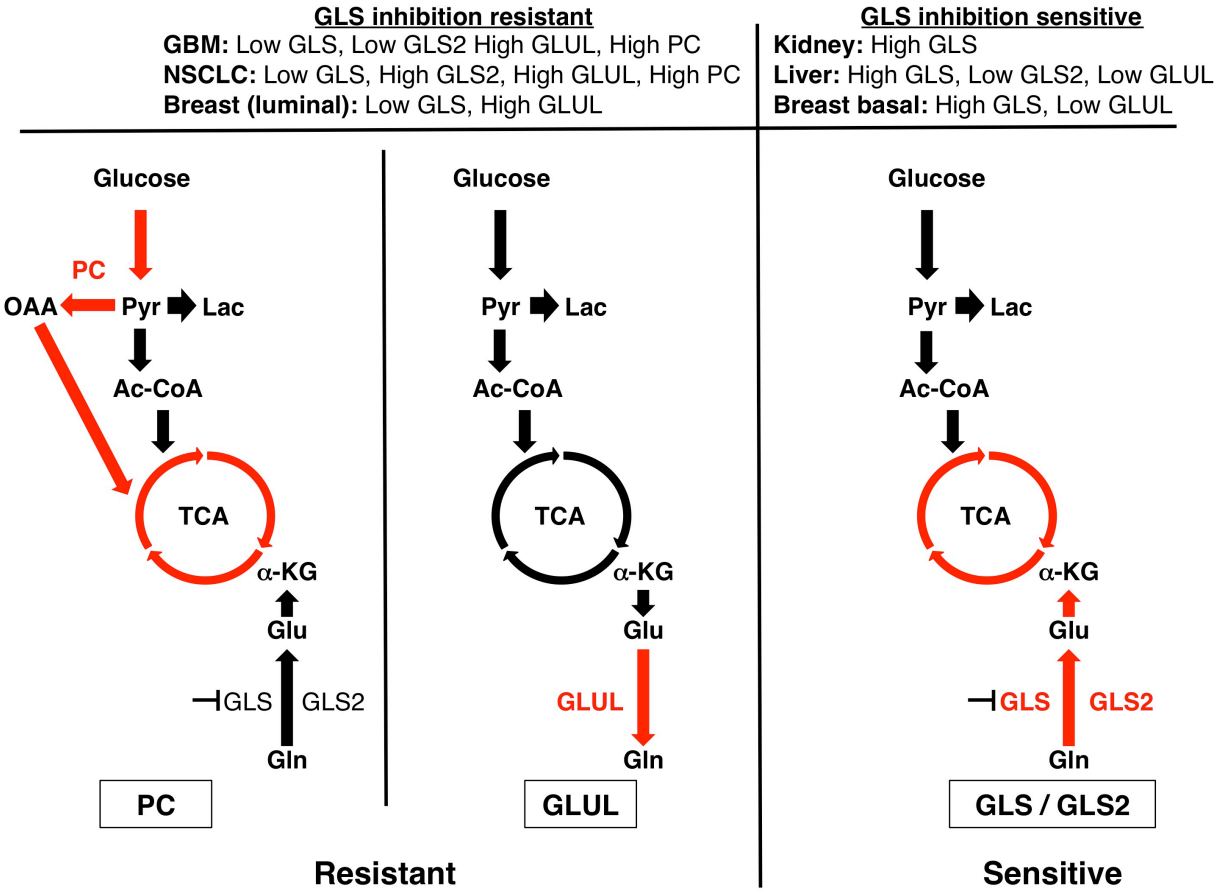
GLS inhibition resistant
GBM: Low GLS, Low GLS2 High GLUL, High PC
NSCLC: Low GLS, High GLS2, High GLUL, High PC
Breast (luminal): Low GLS, High GLUL
GLS inhibition sensitive
Kidney: High GLS
Liver: High GLS, Low GLS2, Low GLUL
Breast basal: High GLS, Low GLUL
Glucose
PC
OAA
Pyr
Lac
Ac-CoA
TCA
α-KG
Glu
GLS
GLS2
Gln
PC
Glucose
Pyr
Lac
Ac-CoA
TCA
α-KG
Glu
GLUL
Gln
GLUL
Resistant
Glucose
Pyr
Lac
Ac-CoA
TCA
α-KG
Glu
GLS
GLS2
Gln
GLS / GLS2
Sensitive

Table 1.1. Glutaminase inhibition across different cancer types *ex vivo* and *in vivo*.

Tumor type	GLS inhibition		Experimental Models
	ex vivo	***in vivo***	
NSCLC (Lung)	Sensitive	Resistant	GEMs and xenografts
GBM	Resistant	Resistant	Patient derived xenografts
Kidney		Sensitive	Transgenic MYC Mice
Liver		Sensitive	Transgenic mice
Breast (luminal)	Resistant		
Breast (Basal)	Sensitive	Sensitive	xenografts
T cell ALL	Sensitive	Sensitive	NOTCH1-induced T-ALL mice
Prostate	Sensitive (+metformin)	Sensitive (+metformin)	Transgenic (TRAMP) mice
Pancreas	Sensitive, sensitizes cells to β-lap treatment	Sensitive, sensitizes cells to β-lap treatment	KRAS induced PDAC xenografts, β-lapachone (β-lap)
Fibrosarcoma	Sensitive (+IKKβ)	Sensitive (+IKKβ)	xenografts, IκB kinase β (IKKβ)

Metabolic phenotype varies with cancer subtype and microenvironment

Different mammalian organs exhibit distinct modes of glutamine metabolism. For example, the kidney mediates net glutamine catabolism, generating ammonia for pH homeostasis and supplying carbon for renal gluconeogenesis [32], whereas lung, skeletal muscle, and adipose tissues exhibit net *de novo* glutamine synthesis *via* the enzyme glutamine synthetase (GLUL) [33]. Similarly, human tumors show a range of metabolic phenotypes that vary with the tissue of origin, the cancer subtype, and the tumor microenvironment.

Although mammalian cells can synthesize glutamine *de novo* using GLUL [34], some cancer cells do not express high levels of *GLUL* and instead are dependent on an exogenous supply of glutamine, which can be catabolized in mitochondria *via* GLS. There is strong evidence that GLS plays an important role in the development of a range of cancers *in vivo*. While data in The Cancer Genome Atlas (TCGA) indicate that the *GLS* transcript is *downregulated* relative to surrounding healthy tissue in NSCLC, consistent with the studies described above, *GLS* mRNA levels are frequently *upregulated* in several other human malignancies (Figure 1.2.). These include tumors of the colon, esophagus, liver, stomach, thyroid, as well as head and neck cancer. In conditional transgenic mouse models, overexpression of the *MYC* proto-oncogene in kidney or liver results in the formation of tumors in which GLS levels are highly upregulated relative to the surrounding healthy tissue [16, 17]. In both of these animal models, inhibition of GLS impedes tumor progression, and deletion of one *GLS* allele in the liver model significantly delays early tumor progression.

In contrast, glutamine *synthesis* is upregulated in some cancers. As outlined above, GLS is dispensable for growth of NSCLC tumors *in vivo* [15], and NSCLC tumors can actually accumulate newly synthesized glutamine [35]. Similarly, some human glioblastoma (GBM)

tumors do not significantly catabolize glutamine *via* GLS and the TCA cycle, but instead accumulate large pools of glutamine, synthesized by GLUL from glucose-derived carbon [36]. This glutamine feeds *de novo* purine biosynthesis, and renders GBM cells self-sufficient for glutamine requirements [34]. Consistent with this metabolic phenotype, GLUL and PC are expressed in most GBM tumors, whereas *GLS* expression is downregulated relative to surrounding brain tissue [34, 36].

Even among tumors that arise in a specific organ, different cancer subtypes can show distinct patterns of glutamine metabolism. Luminal breast cancers frequently exhibit high *GLUL* and low *GLS* expression, whereas the opposite is true of basal breast cancers [19]. Matching these expression patterns, most luminal breast cancer cells can be cultured in glutamine-free media, whereas basal cells are highly sensitive to glutamine withdrawal and to inhibition of GLS, both in cell culture and when grown as xenograft tumors *in vivo* [10, 19]. Metabolic heterogeneity can also arise between different regions of the same tumor. For example, highly perfused regions of NSCLC tumors oxidize diverse nutrients to fuel the TCA cycle, whereas less perfused regions primarily utilize glucose-derived carbon [14].

Thus, some tumors that arise in some tissues are typically dependent on glutamine anaplerosis, whereas NSCLC and GBM more frequently rely on pyruvate anaplerosis to maintain TCA cycle flux (Figure 1.2.). A recent study using the mouse breast cancer cell line 4T1, which metastasizes to the lung with nearly 100% penetrance within a time frame of a day, sheds some light on the factors that influence choice of anaplerotic substrate. In contrast to primary breast tumors, lung metastases were found to rely on PC for TCA cycle anaplerosis, indicating that the tissue microenvironment might favor one metabolic phenotype over another [37]. Supporting this notion, the pyruvate/glutamine ratio is approximately 3-fold higher in the interstitial fluid of the

lungs than in blood plasma, and the pyruvate concentration and expression level of *PC* in breast cancer lung metastases are elevated relative to primary breast tumors [37]. When cultured *ex vivo*, cell lines established from the lung metastases reverted to low levels of PC-dependent anaplerosis, similar to the parental cell line, again illustrating the effect of environment on metabolic phenotype [38]. Nevertheless, cell lines established from 4T1 metastases in different organs do retain some distinctions in their gene expression and metabolic profiles, indicating that adaptation to the microenvironmental nutrient supply does not fully explain the metabolic reprogramming that occurs during metastasis [38]. Another factor that may alter metabolism in the tumor microenvironment is the state of the immune compartment in the tumor. Recent reports have shown that cancer cells can compete with T cells for glucose within the tumor microenvironment and the resulting glucose limitation in T cells suppresses anti-tumor immunity[39, 40]. Given that glutamine metabolism is an important requirement for the metabolism of immune cells (i.e. Immunometabolism)[41-43] a similar effect may occur due to competition for glutamine within the microenvironment.

The impact of oncogenes on glutamine metabolism

Tumors that arise in different organs, but from the same genetic lesion can also have distinct phenotypes for glutamine metabolism. One study demonstrated that *MYC*-induced liver tumors exhibit elevated glutamine catabolism, with increased *GLS* expression and suppressed *GLUL* expression relative to surrounding tissue [17, 35]. In contrast, *MYC*-induced NSCLC tumors exhibit increased expression of *GLUL*, and accumulate glutamine [35]. c-Myc can regulate the expression of both *GLS* and *GLUL* through mechanisms involving suppression of miRNA-23a/b in the case of *GLS*, or upregulation of thymine DNA glycosylase, which leads to

demethylation of, and increased expression from, the *GLUL* gene promoter [44, 45]. These mechanisms serve as examples to potentially explain, albeit non-exhaustively, why c-Myc has contrasting effects on glutamine metabolism in different cellular contexts. Tumors arising within the same tissue, but driven by different oncogenes, can also be metabolically divergent. In contrast to *MYC*-induced liver tumors, *MET*-induced liver tumors lose *GLS* expression, and overexpress *GLUL* and accumulate glutamine [35]. Furthermore, there are many other factors that can regulate glutamine metabolism such as the activity of c-Jun[46], Rb[47, 48], PGC-1/ERRα [49], GLUL acetylation levels [50] and others[4, 6]. Thus, the metabolic phenotype of a given cancer seems to be determined by three key parameters: the tissue of origin, the underlying genetic factors driving tumorigenesis, and the microenvironment.

Tumor glutamine supply

Glutamine can be imported from the microenvironment by the solute carrier (SLC) group of transporters, including members of the SLC1, SLC6, SLC7, SLC36, and SLC38 families. The Na^+/amino acid exchanger SLC1A5 and the unidirectional Na^+/Cl^-/amino acid symporter SLC6A14 are both regulated by c-Myc, and are overexpressed in several cancers [51]. Certain tumors such as pancreatic ductal adenocarcinoma (PDAC) are typically poorly vascularized, and consequently do not have an abundant serum supply of glutamine [52]. PDAC cells instead can in some cases use macropinocytosis to engulf extracellular proteins, which are then degraded in lysosomes to release glutamine and other amino acids [52-55]. An alternative route for cancer cell glutamine supply involves delivery of amino acids *via* extracellular vesicles shed by neighboring cells into the tumor microenvironment. Both PDAC and prostate cancer cells can grow in nutrient-deprived conditions when supplied with amino acids by exosomes shed by

cancer-associated fibroblasts (CAFs) [56]. Additionally, recent work using ovarian carcinoma mouse models uncovered a reliance of cancer cells on stromal CAFs to maintain growth when glutamine is scarce. These fibroblasts boost glutamine synthesis from atypical sources to feed adjacent cancer cells [57]. Nevertheless, tumors that utilize macropinocytosis or uptake extracellular vesicles to acquire glutamine may still require glutaminase and exhibit sensitivity to its inhibition[20, 58].

The metabolic fate of glutamate in cancer

The first step of glutamine catabolism is its conversion to glutamate, which is catalyzed by cytosolic glutamine amidotransferases or by mitochondrial glutaminases. Glutamine-derived glutamate has diverse fates in proliferating cells, including consumption during protein synthesis, supplying nitrogen for transamination reactions, secretion from the cell in exchange for other nutrients, incorporation into the antioxidant tripeptide glutathione, and conversion into α-KG for TCA cycle anaplerosis. Formation of α-KG is catalyzed by the glutamate dehydrogenases (GLUD1/2), which release ammonia as a byproduct, or by transaminases, which transfer the amine-nitrogen of glutamate onto an α-keto acid to generate another amino acid. Some breast cancer cells are known to catabolize glutamate primarily *via* transaminases, thus conserving the amine nitrogen [59]. Alanine transaminase 2 (GPT2), in particular, is critical for α-KG generation and therefore for glutamine/glutamate-mediated TCA cycle anaplerosis in colon cancer cells [60, 61]. In contrast to proliferative cells, transaminase expression is low in quiescent cells, and instead *GLUD* expression is induced [62].

Another major fate of glutamine-derived glutamate is *efflux* from the cell, and glutamine consumption is closely mirrored by glutamate release across the NCI-60 panel of cell lines [25].

The transporter SLC7A11 mediates exchange of intracellular glutamate for extracellular cystine, which, once inside the cell, is reduced to cysteine, the rate-limiting amino acid for glutathione biosynthesis [51]. Expression of the *SLC7A11* gene is induced by c-Myc, and is upregulated in a number of cancers [24]. In addition to the important role of cystine import for redox homeostasis, in some tumors the secreted glutamate can stimulate proliferation by acting on metabotropic and ionotropic glutamate receptors [51].

Epigenetics and signaling

Underlying some of the connections between tumor tissue-of-origin, microenvironment, and metabolic phenotype, is the tumor epigenetic landscape. The connection between metabolism and epigenetics has been better appreciated in recent years [63, 64]. Glucose metabolism, as I will discuss in more detail in the next chapter, has been connected to many epigenetic and posttranslational modifications (PTMs), such as histone and protein acetylation, DNA and histone methylation and many other PTMs. However, given the importance of glutamine in various crucial metabolic pathways, it is not surprising that it is also an important link between metabolism and various epigenetic and post-translational marks. Many epigenetic modifications and processes are regulated by glutamine-derived metabolites including α-KG, which is a cofactor for Jumonji-domain-containing histone demethylases [63]. In a variety of xenograft tumors, the poorly vascularized tumor core shows a selective deficiency of glutamine relative to other amino acids, and a corresponding depletion of glutamine-derived α-KG [27]. This results in an inhibition of α-KG-dependent histone demethylation of H3K27 loci by a Jumonji-domain containing histone demethylase. Consequently, the tumor core exhibits pronounced histone hypermethylation, leading to suppressed expression of differentiation-related

genes and cancer cell dedifferentiation. Additionally, downstream metabolites such as succinate, fumarate and the oncometabolite 2-hydroxyglutarate (2-HG), which arises from mutated isocitrate dehydrogenase 1/2 (IDH1/2) in gliomas and acute myeloid leukemias, can all inhibit these same demethylases [65]. Interestingly, a recent study found that histone hypermethylation can be induced in ^{V600E}*BRAF* melanoma cells by withdrawing glutamine, and the consequent changes in gene expression lead to resistance to BRAF inhibitor treatment [27]. This mechanistic link between glutamine levels and gene-regulatory chromatin changes has important implications for the development of targeted cancer treatments. Inhibition of GLS is currently being evaluated in clinical trials (see below), and might be expected to trigger a histone hypermethylation phenotype that can lead to drug resistance following depletion of glutamine-derived α-KG. Although this suggests a possible mode of resistance to GLS-targeted therapies, it also points towards potential drug synergies that could be exploited in combination treatments. For example, the drug metformin has been identified to have a profound impact on fuel dependence in cancer cells, as it can decrease glucose oxidation and increase glutamine dependency in prostate cancers both *ex vivo* and *in vivo* [21, 28]. Furthermore, glutamine can contribute to the intracellular acetyl-CoA pool as well as to NAD/NADH levels, suggesting a potential role in regulating histone and protein acetylation levels and patterns. Moreover, it has also been shown that UDP-glucosamine (UDP-GlcNAc), used for N-acetylglucosamination (GlcNAcylation) of histones and proteins and can regulate gene expression [66], can be synthesized from glutamine and can also be modulated by it through hexosamine biosynthesis via mTORC2 [67, 68].

Additionally, glutathione (GSH) can inhibit the activity of S-adenosyl methionine synthetase (MAT1A), a key enzyme in the synthesis of S-adenosyl methionine (SAM), the main methyl donor in the cell [69]. It has recently been reported that histone H3 can be S-

glutathionated on Cyc110, which can cause changes in nucleosome stability and alter chromatin structure. Interestingly this modification was observed to increase in proliferating cells relative to quiescent cells [70] Together, this indicates a critical role for glutamine metabolism in regulating and controlling a wide array of epigenetic and PTM marks.

In addition to influencing gene expression *via* epigenetic mechanisms, recent work has implicated glutamine as a signaling agent that can promote cancer progression independently of its metabolic role. As an example, *extracellular* glutamine was recently shown to activate the transcription factor STAT3 to promote cancer cell proliferation [71]. Intracellular glutamine as well can stimulate cell signaling pathways, indirectly activating the mechanistic target of rapamycin complex 1 (mTORC1) [72]. Furthermore, efflux of intracellular glutamine *via* SLC7A5 can drive leucine uptake, another amino acid that is required for mTORC1 activation [73]. Recent work has also connected glutamine metabolism to NOTCH signaling in acute lymphoblastic leukemia (ALL). Inhibiting glutaminolysis and autophagy synergistically enhances the antileukemic effects of anti-NOTCH1 therapies, providing another example of the importance of glutamine metabolism *in vivo* [18].

Targeting glutamine metabolism for cancer therapy

The diverse roles played by glutamine in proliferating cells, supplying carbon and reduced nitrogen for biosynthetic reactions and redox homeostasis, present opportunities for targeting glutamine metabolism for cancer therapy [74]. A number of approaches are conceivable, including depletion of glutamine in blood serum, blockade of cellular glutamine uptake, and inhibition of enzymes involved in glutamine synthesis or catabolism [62]. L-asparaginases, which are routinely used to treat ALL patients, catalyze the deamidation of both asparagine and

glutamine, leading to depletion of both of these amino acids in serum [75]. Since most ALL cells are auxotrophic for asparagine, L-asparaginase effectively starves them of this nutrient. The glutamine hydrolysis activity of L-asparaginases is also thought to contribute to their cytotoxicity, in part because glutamine is required for *de novo* synthesis of asparagine by asparagine synthetase, one potential resistance mechanism to asparagine starvation [75].

Early clinical trials of glutamine antimetabolites revealed unacceptable systemic toxicity, indicating that more selective approaches, for example by defining the tumors that might respond to lower doses, are required to disrupt glutamine metabolism in cancer patients [76]. Two classes of GLS inhibitors have been identified, based on the lead compound molecules '968' and BPTES [11, 12]. The only potential drug to progress beyond preclinical studies, to our knowledge, is the inhibitor CB-839, which is currently being evaluated in Phase I clinical trials [8]. CB-839 is based on the BPTES scaffold, has an IC_{50} value against recombinant human GLS of <50 nM [10], and has shown efficacy against cultured cancer cell lines and xenograft models for triple-negative breast cancer and multiple myeloma [9, 10, 59]. Consistent with studies showing that GLS-mediated glutamine catabolism is required for *in vivo* growth of some tumor types but not others, only certain cancers are sensitive to GLS inhibition, and selection of appropriate target patient groups for CB-839 treatment is essential [8]. Efforts to develop small-molecule inhibitors of the GLS2 isozyme have been limited, presumably because of the conflicting literature reports concerning the importance of this enzyme in cancer. However, lead compounds with sub-micromolar IC_{50} values against recombinant GLS2 were recently identified, and inhibit growth of liver and lung cancer cell lines [77]. It remains to be seen whether GLS2 could be targeted for treatment of tumors such as neuroblastoma, which frequently exhibit elevated *GLS2* expression downstream of N-Myc.

A number of other nodes of cellular glutamine/glutamate metabolism have been proposed as attractive targets for cancer therapy, including transaminases [78], glutamine and glutamate transporters [51], asparagine synthetase [79], and glutamate dehydrogenase [80]. However, to date, studies remain preclinical and there is a lack of potent and selective inhibitors of these proteins, although each of these targets has scientific promise[74].

Concluding Remarks

Our understanding of the roles played by glutamine in cancer is evolving rapidly, and recent work has provided new insights and also has raised a number of questions. It is now clear that there is a not a single 'metabolic map' or 'metabolic switch' describing cancer cell metabolism [81], and the fate of glutamine varies with a range of parameters, including the tissue of origin of a cancer, the genetic aberrations which drive it, the tumor microenvironment, and possibly diet and host metabolism. The collective effect of these variables is striking, such that the metabolic phenotypes of cancer cells range from those that are highly dependent on catabolism of exogenous glutamine, to those that accumulate glutamine *via de novo* synthesis and are self-sufficient for glutamine requirements. Adding an additional level of complexity, recent studies have demonstrated that metabolic phenotype can change when cancer cells are transitioned between different culture systems, or between *ex vivo* cell culture and *in vivo* animal model environments. Standard cell culture media contain excesses of certain nutrients relative to their physiological concentrations, while completely lacking other nutrients such as acetate or aspartate which can play important roles in tumor metabolism [82]. However, these variables are controllable, and we anticipate that future studies will further characterize how metabolic phenotype responds to changing nutrient availability. We also anticipate that advances in

metabolic labeling and modeling methods [37, 83-87], as well as the development of subcellular compartment-specific metabolite isolation methods [88], will reveal new insights into the compartmentalization of glutamine metabolism in cancer cells.

Although the glutamine dependence of some NSCLC cells is lost when they are grown *in vivo*, the canonical anaplerotic role of glutamine prevails in other contexts *in vivo* [9, 10, 12, 16-18, 31], and clinical trials of the GLS inhibitor CB-839 have yielded some promising results [8] suggesting that these recent observations in NSCLC models is certainly not general to all cancers. It is also important to note that the dispensability of glutamine in certain circumstances does not imply that anaplerosis in these cells is not required; as discussed above, cancer cells can find alternative ways to maintain an anaplerotic flux. Continued progress in targeting glutamine metabolism for cancer therapy will likely require identification of synergistic drug combinations along with careful selection of appropriate target patient groups, which could be aided by new techniques for imaging tumor glutamine metabolism *in vivo* [89-92]. Collectively, recent findings on the complexities of cancer cell glutamine metabolism *in vivo* and *ex vivo*, far from 'completing' the field, have generated many new questions, and set the scene for future studies to provide novel and biologically relevant insights.

References:

1. Pavlova, N.N. and C.B. Thompson, *The Emerging Hallmarks of Cancer Metabolism.* Cell Metab, 2016. **23**(1): p. 27-47.
2. DeBerardinis, R.J. and N.S. Chandel, *Fundamentals of cancer metabolism.* Sci Adv, 2016. **2**(5): p. e1600200.
3. Boroughs, L.K. and R.J. DeBerardinis, *Metabolic pathways promoting cancer cell survival and growth.* Nat Cell Biol, 2015. **17**(4): p. 351-9.
4. Nagarajan, A., P. Malvi, and N. Wajapeyee, *Oncogene-directed alterations in cancer cell metabolism.* Trends Cancer, 2016. **2**(7): p. 365-377.
5. Liberti, M.V. and J.W. Locasale, *The Warburg Effect: How Does it Benefit Cancer Cells?* Trends Biochem Sci, 2016. **41**(3): p. 211-8.
6. Altman, B.J., Z.E. Stine, and C.V. Dang, *From Krebs to clinic: glutamine metabolism to cancer therapy.* Nat Rev Cancer, 2016.
7. Jiang, L., et al., *Reductive carboxylation supports redox homeostasis during anchorage-independent growth.* Nature, 2016. **532**(7598): p. 255-8.
8. Garber, K., *Cancer anabolic metabolism inhibitors move into clinic.* Nat Biotechnol, 2016. **34**(8): p. 794-5.
9. Bromley-Dulfano, S., et al., *Antitumor Activity Of The Glutaminase Inhibitor CB-839 In Hematological Malignances.* Blood, 2013. **122**(21): p. 4226-4226.
10. Gross, M.I., et al., *Antitumor activity of the glutaminase inhibitor CB-839 in triple-negative breast cancer.* Mol Cancer Ther, 2014. **13**(4): p. 890-901.
11. Robinson, M.M., et al., *Novel mechanism of inhibition of rat kidney-type glutaminase by bis-2-(5-phenylacetamido-1,2,4-thiadiazol-2-yl)ethyl sulfide (BPTES).* Biochem J, 2007.

406(3): p. 407-14.

12. Wang, J.B., et al., *Targeting mitochondrial glutaminase activity inhibits oncogenic transformation.* Cancer Cell, 2010. **18**(3): p. 207-19.

13. Hosios, A.M., et al., *Amino Acids Rather than Glucose Account for the Majority of Cell Mass in Proliferating Mammalian Cells.* Dev Cell, 2016. **36**(5): p. 540-9.

14. Hensley, C.T., et al., *Metabolic Heterogeneity in Human Lung Tumors.* Cell, 2016. **164**(4): p. 681-94.

15. Davidson, S.M., et al., *Environment Impacts the Metabolic Dependencies of Ras-Driven Non-Small Cell Lung Cancer.* Cell Metab, 2016. **23**(3): p. 517-28.

16. Shroff, E.H., et al., *MYC oncogene overexpression drives renal cell carcinoma in a mouse model through glutamine metabolism.* Proc Natl Acad Sci U S A, 2015. **112**(21): p. 6539-44.

17. Xiang, Y., et al., *Targeted inhibition of tumor-specific glutaminase diminishes cell-autonomous tumorigenesis.* J Clin Invest, 2015. **125**(6): p. 2293-306.

18. Herranz, D., et al., *Metabolic reprogramming induces resistance to anti-NOTCH1 therapies in T cell acute lymphoblastic leukemia.* Nat Med, 2015. **21**(10): p. 1182-9.

19. Kung, H.N., J.R. Marks, and J.T. Chi, *Glutamine synthetase is a genetic determinant of cell type-specific glutamine independence in breast epithelia.* PLoS Genet, 2011. **7**(8): p. e1002229.

20. Son, J., et al., *Glutamine supports pancreatic cancer growth through a KRAS-regulated metabolic pathway.* Nature, 2013. **496**(7443): p. 101-5.

21. Fendt, S.M., et al., *Metformin decreases glucose oxidation and increases the dependency of prostate cancer cells on reductive glutamine metabolism.* Cancer Res, 2013. **73**(14): p.

4429-38.

22. Chakrabarti, G., et al., *Targeting glutamine metabolism sensitizes pancreatic cancer to PARP-driven metabolic catastrophe induced by ss-lapachone.* Cancer Metab, 2015. **3**: p. 12.

23. Reid, M.A., et al., *IKKbeta promotes metabolic adaptation to glutamine deprivation via phosphorylation and inhibition of PFKFB3.* Genes Dev, 2016. **30**(16): p. 1837-51.

24. Eagle, H., *Nutrition needs of mammalian cells in tissue culture.* Science, 1955. **122**(3168): p. 501-14.

25. Jain, M., et al., *Metabolite profiling identifies a key role for glycine in rapid cancer cell proliferation.* Science, 2012. **336**(6084): p. 1040-4.

26. Timmerman, L.A., et al., *Glutamine sensitivity analysis identifies the xCT antiporter as a common triple-negative breast tumor therapeutic target.* Cancer Cell, 2013. **24**(4): p. 450-65.

27. Pan, M., et al., *Regional glutamine deficiency in tumours promotes dedifferentiation through inhibition of histone demethylation.* Nat Cell Biol, 2016. **18**(10): p. 1090-1101.

28. Liu, X., et al., *Metformin Targets Central Carbon Metabolism and Reveals Mitochondrial Requirements in Human Cancers.* Cell Metab, 2016. **24**(5): p. 728-739.

29. Sellers, K., et al., *Pyruvate carboxylase is critical for non-small-cell lung cancer proliferation.* J Clin Invest, 2015. **125**(2): p. 687-98.

30. Cheng, T., et al., *Pyruvate carboxylase is required for glutamine-independent growth of tumor cells.* Proc Natl Acad Sci U S A, 2011. **108**(21): p. 8674-9.

31. Matre, P., et al., *Inhibiting glutaminase in acute myeloid leukemia: metabolic dependency of selected AML subtypes.* Oncotarget, 2016.

32. Stumvoll, M., et al., *Role of glutamine in human carbohydrate metabolism in kidney and other tissues.* Kidney Int, 1999. **55**(3): p. 778-92.

33. Hensley, C.T., A.T. Wasti, and R.J. DeBerardinis, *Glutamine and cancer: cell biology, physiology, and clinical opportunities.* J Clin Invest, 2013. **123**(9): p. 3678-84.

34. Tardito, S., et al., *Glutamine synthetase activity fuels nucleotide biosynthesis and supports growth of glutamine-restricted glioblastoma.* Nat Cell Biol, 2015. **17**(12): p. 1556-68.

35. Yuneva, M.O., et al., *The metabolic profile of tumors depends on both the responsible genetic lesion and tissue type.* Cell Metab, 2012. **15**(2): p. 157-70.

36. Marin-Valencia, I., et al., *Analysis of tumor metabolism reveals mitochondrial glucose oxidation in genetically diverse human glioblastomas in the mouse brain in vivo.* Cell Metab, 2012. **15**(6): p. 827-37.

37. Christen, S., et al., *Breast Cancer-Derived Lung Metastases Show Increased Pyruvate Carboxylase-Dependent Anaplerosis.* Cell Rep, 2016. **17**(3): p. 837-848.

38. Dupuy, F., et al., *PDK1-Dependent Metabolic Reprogramming Dictates Metastatic Potential in Breast Cancer.* Cell Metab, 2015. **22**(4): p. 577-89.

39. Chang, C.H., et al., *Metabolic Competition in the Tumor Microenvironment Is a Driver of Cancer Progression.* Cell, 2015. **162**(6): p. 1229-41.

40. Ho, P.C., et al., *Phosphoenolpyruvate Is a Metabolic Checkpoint of Anti-tumor T Cell Responses.* Cell, 2015. **162**(6): p. 1217-28.

41. Nakaya, M., et al., *Inflammatory T cell responses rely on amino acid transporter ASCT2 facilitation of glutamine uptake and mTORC1 kinase activation.* Immunity, 2014. **40**(5): p. 692-705.

42. Blagih, J., et al., *The energy sensor AMPK regulates T cell metabolic adaptation and effector responses in vivo.* Immunity, 2015. **42**(1): p. 41-54.

43. O'Neill, L.A., R.J. Kishton, and J. Rathmell, *A guide to immunometabolism for immunologists.* Nat Rev Immunol, 2016. **16**(9): p. 553-65.

44. Gao, P., et al., *c-Myc suppression of miR-23a/b enhances mitochondrial glutaminase expression and glutamine metabolism.* Nature, 2009. **458**(7239): p. 762-5.

45. Bott, A.J., et al., *Oncogenic Myc Induces Expression of Glutamine Synthetase through Promoter Demethylation.* Cell Metab, 2015. **22**(6): p. 1068-77.

46. Lukey, M.J., et al., *The oncogenic transcription factor c-Jun regulates glutaminase expression and sensitizes cells to glutaminase-targeted therapy.* Nat Commun, 2016. **7**: p. 11321.

47. Nicolay, B.N., et al., *Loss of RBF1 changes glutamine catabolism.* Genes Dev, 2013. **27**(2): p. 182-96.

48. Reynolds, M.R., et al., *Control of glutamine metabolism by the tumor suppressor Rb.* Oncogene, 2014. **33**(5): p. 556-66.

49. McGuirk, S., et al., *PGC-1alpha supports glutamine metabolism in breast cancer.* Cancer Metab, 2013. **1**(1): p. 22.

50. Nguyen, T.V., et al., *Glutamine Triggers Acetylation-Dependent Degradation of Glutamine Synthetase via the Thalidomide Receptor Cereblon.* Mol Cell, 2016. **61**(6): p. 809-20.

51. Bhutia, Y.D., et al., *Amino Acid transporters in cancer and their relevance to "glutamine addiction": novel targets for the design of a new class of anticancer drugs.* Cancer Res, 2015. **75**(9): p. 1782-8.

52. Kamphorst, J.J., et al., *Human pancreatic cancer tumors are nutrient poor and tumor cells actively scavenge extracellular protein.* Cancer Res, 2015. **75**(3): p. 544-53.

53. Commisso, C., et al., *Macropinocytosis of protein is an amino acid supply route in Ras-transformed cells.* Nature, 2013. **497**(7451): p. 633-7.

54. Palm, W., et al., *The Utilization of Extracellular Proteins as Nutrients Is Suppressed by mTORC1.* Cell, 2015. **162**(2): p. 259-70.

55. Davidson, S.M., et al., *Direct evidence for cancer-cell-autonomous extracellular protein catabolism in pancreatic tumors.* Nat Med, 2016.

56. Zhao, H., et al., *Tumor microenvironment derived exosomes pleiotropically modulate cancer cell metabolism.* Elife, 2016. **5**: p. e10250.

57. Yang, L., et al., *Targeting Stromal Glutamine Synthetase in Tumors Disrupts Tumor Microenvironment-Regulated Cancer Cell Growth.* Cell Metab, 2016. **24**(5): p. 685-700.

58. Santana, S.M., et al., *Cancerous epithelial cell lines shed extracellular vesicles with a bimodal size distribution that is sensitive to glutamine inhibition.* Phys Biol, 2014. **11**(6): p. 065001.

59. Coloff, J.L., et al., *Differential Glutamate Metabolism in Proliferating and Quiescent Mammary Epithelial Cells.* Cell Metab, 2016. **23**(5): p. 867-80.

60. Smith, B., et al., *Addiction to Coupling of the Warburg Effect with Glutamine Catabolism in Cancer Cells.* Cell Rep, 2016. **17**(3): p. 821-836.

61. Hao, Y., et al., *Oncogenic PIK3CA mutations reprogram glutamine metabolism in colorectal cancer.* Nat Commun, 2016. **7**: p. 11971.

62. Lukey, M.J., K.F. Wilson, and R.A. Cerione, *Therapeutic strategies impacting cancer cell glutamine metabolism.* Future Med Chem, 2013. **5**(14): p. 1685-700.

63. Kinnaird, A., et al., *Metabolic control of epigenetics in cancer.* Nat Rev Cancer, 2016.

64. Gao, X., et al., *Metabolic interactions with cancer epigenetics.* Mol Aspects Med, 2016.

65. Dang, L., K. Yen, and E.C. Attar, *IDH mutations in cancer and progress toward development of targeted therapeutics.* Ann Oncol, 2016. **27**(4): p. 599-608.

66. Hanover, J.A., M.W. Krause, and D.C. Love, *Bittersweet memories: linking metabolism to epigenetics through O-GlcNAcylation.* Nat Rev Mol Cell Biol, 2012. **13**(5): p. 312-21.

67. Moloughney, J.G., et al., *mTORC2 Responds to Glutamine Catabolite Levels to Modulate the Hexosamine Biosynthesis Enzyme GFAT1.* Mol Cell, 2016. **63**(5): p. 811-26.

68. Ferrer, C.M., V.L. Sodi, and M.J. Reginato, *O-GlcNAcylation in Cancer Biology: Linking Metabolism and Signaling.* J Mol Biol, 2016. **428**(16): p. 3282-94.

69. Garcia-Gimenez, J.L. and F.V. Pallardo, *Maintenance of glutathione levels and its importance in epigenetic regulation.* Front Pharmacol, 2014. **5**: p. 88.

70. Garcia-Gimenez, J.L., et al., *Histone h3 glutathionylation in proliferating mammalian cells destabilizes nucleosomal structure.* Antioxid Redox Signal, 2013. **19**(12): p. 1305-20.

71. Cacace, A., et al., *Glutamine activates STAT3 to control cancer cell proliferation independently of glutamine metabolism.* Oncogene, 2016.

72. Jewell, J.L., et al., *Metabolism. Differential regulation of mTORC1 by leucine and glutamine.* Science, 2015. **347**(6218): p. 194-8.

73. Nicklin, P., et al., *Bidirectional transport of amino acids regulates mTOR and autophagy.* Cell, 2009. **136**(3): p. 521-34.

74. Martinez-Outschoorn, U.E., et al., *Cancer metabolism: a therapeutic perspective.* Nat Rev Clin Oncol, 2016.

75. Covini, D., et al., *Expanding targets for a metabolic therapy of cancer: L-asparaginase.* Recent Pat Anticancer Drug Discov, 2012. **7**(1): p. 4-13.

76. Ahluwalia, G.S., et al., *Metabolism and action of amino acid analog anti-cancer agents.* Pharmacol Ther, 1990. **46**(2): p. 243-71.

77. Lee, Y.Z., et al., *Discovery of selective inhibitors of Glutaminase-2, which inhibit mTORC1, activate autophagy and inhibit proliferation in cancer cells.* Oncotarget, 2014. **5**(15): p. 6087-101.

78. Korangath, P., et al., *Targeting Glutamine Metabolism in Breast Cancer with Aminooxyacetate.* Clin Cancer Res, 2015. **21**(14): p. 3263-73.

79. Gutierrez, J.A., et al., *An inhibitor of human asparagine synthetase suppresses proliferation of an L-asparaginase-resistant leukemia cell line.* Chem Biol, 2006. **13**(12): p. 1339-47.

80. Jin, L., et al., *Glutamate dehydrogenase 1 signals through antioxidant glutathione peroxidase 1 to regulate redox homeostasis and tumor growth.* Cancer Cell, 2015. **27**(2): p. 257-70.

81. Strickaert, A., et al., *Cancer heterogeneity is not compatible with one unique cancer cell metabolic map.* Oncogene, 2016.

82. Mayers, J.R. and M.G. Vander Heiden, *Famine versus feast: understanding the metabolism of tumors in vivo.* Trends Biochem Sci, 2015. **40**(3): p. 130-40.

83. Park, J.O., et al., *Metabolite concentrations, fluxes and free energies imply efficient enzyme usage.* Nat Chem Biol, 2016. **12**(7): p. 482-9.

84. Hackett, S.R., et al., *Systems-level analysis of mechanisms regulating yeast metabolic flux.* Science, 2016. **354**(6311).

85. Dai, Z. and J.W. Locasale, *Understanding metabolism with flux analysis: From theory to application.* Metab Eng, 2016.

86. Dai, Z., et al., *A Flux Balance of Glucose Metabolism Clarifies the Requirements of the Warburg Effect.* Biophys J, 2016. **111**(5): p. 1088-100.

87. Buescher, J.M., et al., *A roadmap for interpreting (13)C metabolite labeling patterns from cells.* Curr Opin Biotechnol, 2015. **34**: p. 189-201.

88. Chen, W.W., et al., *Absolute Quantification of Matrix Metabolites Reveals the Dynamics of Mitochondrial Metabolism.* Cell, 2016. **166**(5): p. 1324-1337 e11.

89. Schulte, M.L., et al., *Non-Invasive Glutamine PET Reflects Pharmacological Inhibition of BRAFV600E In Vivo.* Mol Imaging Biol, 2016.

90. Zhang, Y. and J. Shen, *Simultaneous quantification of glutamate and glutamine by J-modulated spectroscopy at 3 Tesla.* Magn Reson Med, 2016. **76**(3): p. 725-32.

91. Venneti, S., et al., *Glutamine-based PET imaging facilitates enhanced metabolic evaluation of gliomas in vivo.* Sci Transl Med, 2015. **7**(274): p. 274ra17.

92. Hassanein, M., et al., *Preclinical Evaluation of 4-[18F]Fluoroglutamine PET to Assess ASCT2 Expression in Lung Cancer.* Mol Imaging Biol, 2016. **18**(1): p. 18-23.

CHAPTER 2

[†]Titratable rates of glycolysis quantitatively mediate specific histone acetylation sites

Abstract

Glucose metabolism links metabolic status to protein acetylation. However, it remains poorly understood to what extent do features of glucose metabolism contribute to protein acetylation and whether the process can be dynamically and quantitatively regulated by differing rates of glycolysis. In this chapter, we show that in HCT-116 human colon cancer cells, titratable rates of glycolysis with corresponding changes in the levels of glycolytic intermediates result in a graded remodeling of a bulk of the metabolome and resulted in gradual changes in total histone acetylation levels. Dynamic histone acetylation levels were found and most strongly correlated with acetyl coenzyme A (ac-CoA) levels and inversely associated with the ratio of ac-CoA to free CoA. A multiplexed stable isotopic labeling by amino acids in cell culture (SILAC)-based proteomics approach revealed that the levels of half of identified histone acetylation sites as well as other lysine acylation modifications are tuned by the rate of glycolysis demonstrating that glycolytic rate affects specific acylation sites. We demonstrate that histone acylation is directly sensed by glucose flux in a titratable, dose-dependent manner that is modulated by glycolytic flux and that a possible function of the Warburg Effect, a metabolic state observed in cancers with enhanced glucose metabolism, is to confer specific signaling effects on cells.

[†] Adapted from Cluntun, A.A., Huang, H., Dai, L., Liu, X., Zhao, Y. and Locasale, J.W., (2015) *Cancer Metab.* **3**: p. 10. Author contributions: A.A.C., Y.Z. and J.W.L designed the study. A.A.C. and J.W.L wrote the paper. A.A.C maintained the cell cultures, performed the 2DG treatments, performed the SILAC experiment, collected and analyzed the data, performed the immunoblot assays and made all the figures. A.A.C. and X.L performed the metabolomics experiments and ran metabolites on HPLC/MS/MS. H.H. and L.D. extracted and digested the histone proteins and performed the PTM purification. Y.Z. advised on the acylation proteomics experiments. H.H. ran and analyzed the tryptic peptides.

Introduction:

The metabolism of carbohydrates through glycolysis affects numerous cellular processes through its effects on biosynthetic, energy, and reactive oxygen species metabolism. Glucose metabolism is altered in pathological conditions such as cancer and autoimmunity[1, 2]. In these cases, cells metabolize their glucose under oxygenated conditions, at higher rates, and ferment the glucose to produce lactate that together is referred to as the "Warburg effect" or aerobic glycolysis[3]. There are many hypotheses for the biological function of the Warburg effect[4, 5]. It has been proposed that since glycolysis to lactate occurs at a faster rate than that of oxidative phosphorylation, glycolysis provides a means to generate ATP more rapidly[6, 7]. It has also been proposed that the Warburg effect is an adaptation to support the biosynthetic requirements of cancer cells[8, 9]. Each of these proposals, however, is not without difficulties. For example, estimates have found that over 90% of the carbon from glucose is secreted as lactate and alanine leaving little room for biosynthesis[10]. Also, the rapid ATP produced by glycolysis can also be obtained by other mechanisms such as creatine kinase and adenylate kinase[11, 12].

Additionally, direct biochemical signaling functions of glucose metabolism are also possible[13, 14]. When the rate of glycolytic flux changes, it is likely that the levels of metabolites that serve as intermediates in glycolysis and associated pathways are consequentially altered. Changes in metabolite levels, if they are used as substrates or cofactors for enzymes that carry out posttranslational modifications (PTMs), could allow for metabolism to serve an active role in remodeling cell physiology by altering signaling activities[15-18]. For example, if these PTMs affect the conformation of chromatin, they can potentially alter the expression of thousands of genes. Numerous studies have shown that changes in glucose metabolism can regulate histone acetylation[19-26]. There are multiple molecular links from glucose metabolism to protein

acetylation status including intracellular pH[27]. By this model, pH is mediated by lactate, the product of aerobic glycolysis. Acetyl-coenzyme A (ac-CoA), a product of glycolysis, is the substrate used by acetyltransferases to modify transfer of the ac-CoA moiety to histones. In addition, the free coenzyme A (CoA) product can inhibit these enzymes[28]. Also, the redox status mediated by NAD^+ and NADH can affect the activity of certain deacetylases[29].

Furthermore, ketone bodies, which are produced during fatty acid oxidation, can also inhibit histone deacetylases[29, 30]. Despite these intriguing biochemical clues, it remains unknown how these phenomena coordinate histone modifications and how they are quantitatively mediated. Their specificity regarding defined acetylation sites is also poorly understood. In addition, multiple factors can contribute to the regulation of histone acetylation resulting from altered glucose metabolism, and identifying the critical factors in metabolism that will be important understanding its role in the regulation of histone acetylation. Moreover, recently discovered histone modifications such as histone propionylation, butyrylation and 2-hydroxyisobutyrylation have each been identified as unique histone modifications important for gene expression[31-34]. Much like histone acetylation, these modifications use their corresponding acyl-CoA metabolite species as substrates for the PTM. How glycolytic flux affects the specific pathways that supply the cofactors for these modifications remains unknown. Lastly, it remains unclear how coordinated changes in metabolite concentrations at the systems level employ altered glucose metabolism to affect biologically important histone acetylation.

To test the hypothesis that glycolytic rate alters the levels of metabolites that in turn regulate histone acetylation, we considered a system where we can quantitatively tune the rate of glycolysis and as a result affect the concentrations of metabolites in glycolysis. We then carried out a metabolomics study that considered how differences in metabolite concentrations

quantitatively affect histone acetylation. In measuring each potential contribution to histone acetylation, we found several factors that contribute to this modification. Together these results provide a quantitative model for the contributions of glycolysis to altered histone acetylation and acylation and provide evidence for the direct sensing of glucose metabolism by histone acetylation. Since histone acetylation controls and in part determines the expression of thousands of genes, it is tempting to speculate that this mechanism may provide a general link from metabolism to the remodeling of chromatin in cells.

Materials and Methods

Cell Culture and Reagents. HCT116 colorectal cancer cell lines were cultured in full media composed of RPMI 1640, 10% Fetal Bovine Serum (FBS), 100 U/mL penicillin, and 100mg/mL streptomycin. All cell lines were obtained as gifts from Lewis Cantley's laboratory. Cells were cultured in a 37 °C, 5% CO_2 atmosphere. For 2-Deoxy-d-Glucose (2DG) titration experiments, either 2DG (Sigma) was added to the media at the respective concentrations or 0.01% DMSO (cellgro) for the Vehicle (Veh). At the start of each experiment cells were seeded at a density of 2.2 x 106 cells for 10 cm plates for protein collection or 3 x 10^5 cells/well in a 6-well plate for metabolite collection and allowed to adhere and grow to 80% confluence. Cells were then washed with PBS and allowed to incubate in the respective treatments for 6 hours. Histones and metabolites were extracted as described below.

Immunoblotting. Samples were homogenized in Triton Extraction Buffer (TEB: 0.5% Triton X 100, 2mM Phenylmethylsulfonyl fluoride (PMSF), 0.02% NaN3 in PBS) and centrifuged at 2000rpm for 10 min at 4°C. Pellets were resuspended in 0.2N HCl and histones were acid

extracted overnight at 4°C. Histones were then precipitated in 100% Trichloroacetic acid (TCA) (Sigma-Aldrich), washed with cold Acetone and allowed to air dry. Pellets were either stored at -20 or dissolved in ddH2O. Histone extracts were loaded onto 12% SDS-PAGE gels and transferred to polyvinylidene difluoride (PVDF) membranes. Membranes were blocked in 5% dry milk in TBST and incubated with anti-acetyl-H3K27 (Abcam) 1:2000, anti-acetyl H3 (Millipore) 1:2000, or anti-H3 (Millipore) 1:10000. Horseradish-peroxidase-conjugated anti-rabbit (Rockland), 1:10,000, was used as secondary antibodies. Chemiluminescent signals were detected with Clarity Western ECL Detection Kit (Bio-Rad) and imaged using a ChemiDoc MP System (Bio-Rad).

Metabolite Extraction. The procedures for cultured cells are described in previous studies [35, 36]. Briefly, for culture from adherent cells, the media was quickly aspirated and cells were washed with cold PBS on dry ice. Then, 1mL of extraction solvent (80% methanol/water) cooled to -80°C was added immediately to each well, and the dishes were transferred to -80°C for 15 minutes. Plates were removed and cells were scraped into the extraction solvent on dry ice. All metabolite extracts were centrifuged at 20,000g at 4°C for 10 min. Finally, the solvent in each sample was evaporated in a Speed Vacuum for metabolomics analysis. For polar metabolite analysis, the cell extract was dissolved in 15μL water and 15μL methanol/acetonitrile (1:1 v/v) (LC-MS optima grade, Thermo Scientific). For nonpolar CoA metabolite analysis, the cell extract was dissolved in 50 mM ammonium acetate (pH 6.8). Samples were centrifuged at 20,000g for 10min at 4°C and the supernatants were transferred to Liquid Chromatography (LC) vials. The injection volume for polar metabolite analysis was 8 uL.

U-^{13}C-Glucose labeling. Cells were first cultured in standard RPMI 1640, 10% Fetal Bovine Serum (FBS), 100 U/mL penicillin, and 100mg/mL streptomycin media to 70% confluence. They were then washed with PBS and treated with corresponding 2DG in fresh media as described above and incubated for 6 hours. Subsequently, the cells were washed with PBS and corresponding media conditions where glucose is replaced with U-13C6-D-glucose (Cambridge Isotope Laboratories, Inc.) was considered. Metabolites were then extracted at the indicated time points as described in the text from the spent media.

Liquid Chromatography. For polar metabolites an Xbridge amide column (100 x 2.1 mm i.d., 3.5 μm; Waters) is employed, whereas for nonpolar acyl-CoA metabolites a LUNA C18 column (100 x 2.0 mm; phenomenex) is employed on a Dionex (Ultimate 3000 UHPLC) for compound separation at room temperature. The mobile phase A is 20 mM ammonium acetate and 15 mM ammonium hydroxide in water with 3% acetonitrile, pH 9.0 and mobile phase B is acetonitrile. The linear is as gradient as follows: 0 min, 85% B; 1.5 min, 85% B, 5.5 min, 35% B; 10min, 35% B, 10.5 min, 35% B, 14.5 min, 35% B, 15 min, 85% B, and 20 min, 85% B. The flow rate was 0.15 ml/min from 0 to 10 min and 15 to 20 min, and 0.3 ml/min from 10.5 to 14.5 min. All solvents are LCMS grade and purchased from Fisher Scientific.

Mass spectrometry. The Q Exactive MS (Thermo Scientific) is equipped with a heated electrospray ionization probe (HESI), and the relevant parameters are as listed: evaporation temperature, 120 °C; sheath gas, 30; auxiliary gas, 10; sweep gas, 3; spray voltage, 3.6 kV for positive mode and 2.5 kV for negative mode. Capillary temperature was set at 320°C, and S-lens was 55. A full scan range from 60 to 900 (m/z) was used. The resolution was set at 70,000. The

maximum injection time was 200 ms. Automated gain control (AGC) was targeted at 3,000,000 ions.

Metabolomics and data analysis. Raw data collected from LC-Q Exactive MS is processed on Sieve 2.0 (Thermo Scientific). Peak alignment and detection are performed according to the protocol described by Thermo Scientific. For a targeted metabolite analysis, the method "peak alignment and frame extraction" is applied. An input file of theoretical m/z and detected retention time of 263 known metabolites is used for targeted metabolites analysis with data collected in positive mode, while a separate input file of 197 metabolites is used for negative mode. M/Z width is set at 10 ppm. The output file including detected m/z and relative intensity in different samples is obtained after data processing. Quantitation and statistics were calculated and visualized with Microsoft Excel, Gene-E and MetaboAnalyst online software.

Stable Isotope Labeling by Amino acids in Cell culture (SILAC) Experiments. Heavy lysine ($^{13}C_6{}^{15}N_2$-L-Lysine:2HCL), Medium lysine (4,4,5,5-D4-L-Lysine:2HCL) and RPMI 1640 Media for SILAC (minus L-Lysine and L-Arginine) were purchased from Cambridge Isotope Laboratories, Inc. Light lysine (L-Lysine HCl) and arginine (L-Arginine HCl) were purchased from Amresco. Cells were inoculated into a 6 well plates and allowed to grow for at least 6 doublings in respective SILAC media. Media was replenished every 3 days. Cells were then expanded to 15 cm plates till 80% confluent. Cells were then treated with corresponding 2DG treatments (100uM, 5mM, veh) for 6 hours. (5 mM:heavy lysine, 100 μM:medium lysine, veh:light lysine).

Histone proteins extraction and in-solution digestion. The "heavy", "medium", and "light" labeled cells were washed twice with pre-chilled PBS, and the core histone proteins were prepared using an acid-extraction procedure previously described [37], respectively. Each acid-extracted histone protein solution was clarified by centrifugation for 10 min at 20,000xg. The protein concentrations of the supernatants were measured and equal amounts of proteins from the three pools of cells were combined. Then trypsin (Promega Corp., Madison, WI) was added into the protein mixtures at a trypsin-to-protein ratio of 1:50 (w/w) for digestion at 37 ^{o}C for 16 hours.

PTM specific immunoaffinity purification (IP). To enrich the peptides with specific PTMs (lysine acetylation, lysine propionylation, lysine butyrylation, and lysine 2-hydroxyisobutyrylation), 200 µg of tryptic peptides were incubated with PTM-specific antibody-immobilized beads (containing 20 µg of antibody, PTM Biolabs, Chicago, IL) in NETN buffer (50 mM Tris pH 8.0, 100 mM NaCl, 1 mM EDTA, 0.5% NP40) at 4 °C for 6 hours with gentle rotation. The beads were carefully washed three times with NETN buffer, twice with ETN buffer (50 mM Tris, pH 8.0, 100 mM NaCl, 1 mM EDTA) and once with ddH_2O. After IP, 24.22% (on average) of the total identified peptides are modified. The bound peptides were eluted from the beads with 0.1%TFA in water and vacuum-dried. The resulting peptides were dissolved in 0.5% formic acid-water solution, and desalted with Ziptip C18 (EMD Millipore Corp., Darmstadt, Germany) according to the manufacturer's instructions.

HPLC/MS/MS analysis of tryptic peptides. The desalted samples were dissolved in 2.5 µL HPLC A buffer containing 0.1% formic acid and 99.9% water (v/v). The solution was directly loaded

onto a homemade capillary column (10 cm length with 75 μm inner diameter) packed with Jupiter C12 resin (4 μm particle size, 90 Å pore size, Phenomenex Inc., Torrance, CA) and connected to a NanoLC-1D plus HPLC system (Eksigent Technologies, LLC., Dublin, CA). Peptides were eluted with a gradient of 5% to 90% HPLC buffer B (0.1% formic acid in acetonitrile, v/v) in buffer A (0.1% formic acid in water, v/v) at a flow rate of 300 nL/min over 76 min. The eluted peptides were ionized and introduced into an LTQ-Orbitrap Velos mass spectrometer (Thermo Fisher Scientific Inc., Waltham, MA) using a nanospray source. Full MS scans were acquired in the Orbitrap mass analyzer over the range m/z 300-1800 with a mass resolution of 60000 at m/z 400. The 20 most intense peaks with charge of +2 - +4 were isolated for MS/MS analysis.

SILAC based quantification analysis. Protein and PTM site identification and quantification were performed with MaxQuant version 1.3.0.5 software [38, 39] against Uniprot human reference protein database concatenated with reverse decoy database and protein sequences of common contaminants. Trypsin was specified as cleavage enzyme with 2 and 4 max missed cleavages for protein and PTM site quantification, respectively. Maximum numbers of labeled amino acids were set as 3 and 5 for protein and PTM quantification, respectively. Several variable modifications were selected: oxidation (M), acetylation (protein N-term); acetylation (K), tri-methylation (K), di-methylation (K,R), mono-methylation (K,R), and specific PTM at lysine residues corresponding to each immunoaffinity purification. False discovery rate (FDR) thresholds for protein, peptide and modification sites were specified at 0.01. Minimum peptide length was set at 7 for protein quantification and 5 for PTM site quantification. Identified PTM sites with Andromeda score less than 40 or site localization probability less than 0.75, as well as

site identifications from reverse or contaminant protein sequences were removed. In addition, C-terminal modified peptides were also removed unless located at the peptide C-terminal residue of the corresponding protein. Protein ratios were determined based on a minimum of two peptide ratios using razor and unique peptides. The final PTM site ratios were normalized by their protein ratios.

Results

Development of a system for titratable rates of glucose metabolism

To investigate quantitative mechanisms linking glucose metabolism to histone acetylation, we developed a system where the rates of glucose metabolism and as a result, levels of metabolites could be controlled in a precise manner. One possibility of a tunable system is to consider the incorporation of 2-deoxyglucose (2DG) into cells (Fig. 2.1A). 2DG can affect glycolysis through multiple inhibitory mechanisms. It is taken up in cells via glucose transporters (GLUTs) where it is phosphorylated by hexokinase but cannot be further metabolized in glycolysis by phosphofructoisomerase[40]. At all concentrations, 2DG directly competes with glucose for binding and product inhibition of glucose and glucose-6-phosphate[40-43]. At higher concentrations, 2DG acquires the properties of an inhibitor of hexokinase[44-46]. At intermediate concentrations, a combination of multiple mechanisms that can affect glycolytic rate occur[45, 47]. Thus, differing concentrations of 2DG may exert unique effects on glycolysis (Fig. 2.1A). To exploit these different characteristics, we treated cells with 2DG at different concentration with short incubation times. The short times were considered in order to minimize potential confounding indirect effects of 2DG on cells that occur downstream of glycolysis that

may ensue at longer incubation times. Notably, this timeframe is also sufficiently long for 2DG to enter cells and initiate its mechanism of action. We therefore treated HCT116 cells with six concentrations (0, 0.1, 0.5, 1, 2.5, and 5 mM) of 2DG for a short time (6 hours) that preceded growth arrest and any detectable cell death (Fig. 2.1E). A graded accumulation of glucose in the extracellular media was observed, as unphosphorylated glucose cannot be retained intracellularly[46] (Fig. 2.1B). At these differing concentrations, we next measured the phosphorylated product of 2DG, 2-deoxyglucose-6-phosphate (2DG6P), which accumulates in the cell since its negative charge precludes it from passing through cell membranes, and also observed a dose-dependent accumulation of this product as well[46] (Fig. 2.1C). Furthermore, we employed a kinetic flux profiling experiment using U-^{13}C-glucose and observed a decrease in the production rate of labeled lactate in the medium, further confirming that the system is affecting glycolytic flux directly at differing doses of 2DG treatment (Fig. 2.1D). These results indicate that a gradual change in 2DG dose results in similar incremental changes in glycolytic flux as well as in the levels of metabolites both in glycolysis and more broadly across the

Figure 2.1. The rate of glucose metabolism and extent of metabolic reprogramming can be tuned with pharmacological manipulation.

(A) Schematic of 2DG effects on glycolysis at high vs low concentrations. (B) Relative extracellular glucose levels in response to each 2DG concentration compared to the vehicle (Veh). (C) Relative 2DG6P levels in response to 2DG treatment compared to Veh. (D) Production rate of ^{13}C-labeled lactate in response to 2DG treatment. Fold change in relative amounts of lactate in media after respective treatments is depicted. (E) Cell viability test of HCT-116 cells after 6 hours of growth under indicated treatments. Mean ± SEM of triplicates relative to the Veh. (*P <0.05 relative to Veh)

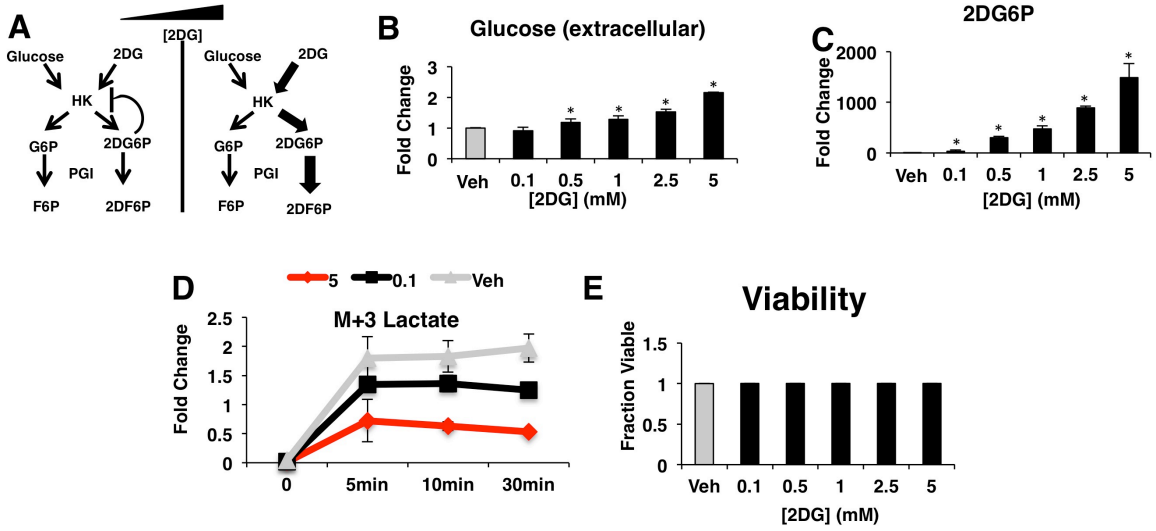
A
[2DG]
Glucose
2DG
HK
G6P
2DG6P
PGI
F6P
2DF6P
Glucose
2DG
HK
G6P
2DG6P
PGI
F6P
2DF6P
B
Glucose (extracellular)
Fold Change
3
2
1
0
Veh
0.1
0.5
1
2.5
5
[2DG] (mM)
C
2DG6P
Fold Change
2000
1000
0
Veh
0.1
0.5
1
2.5
5
[2DG] (mM)
D
5
0.1
Veh
M+3 Lactate
Fold Change
2.5
2
1.5
1
0.5
0
0
5min
10min
30min
E
Viability
Fraction Viable
1.5
1
0.5
0
Veh
0.1
0.5
1
2.5
5
[2DG] (mM)

metabolic network. To investigate how this titratable change in glycolysis globally affected cellular metabolism, we generated a profile of over 300 metabolites using a metabolomics technology we have recently developed based on liquid chromatography coupled to high resolution mass spectrometry[35, 36, 48]. This measurement allows for the quantitation of a diverse spectrum of metabolic pathways including sugar, amino acid, and polar lipid metabolism. Across these different concentrations of 2DG, we observed graded waves of changes in metabolism involving multiple different pathways across the metabolic network (Fig. 2.2A). An inspection of glycolytic intermediates (Fig. 2.2B) revealed a graded response in the depletion of metabolites, whereas, tricarboxylic acid (TCA) cycle (Fig. 2.2C) intermediates displayed a more complex response. Pyruvate exhibited a qualitatively different behavior from that of the other glycolytic intermediates likely due to other sources including lactate and alanine also contributing to pyruvate biosynthesis. Other substrates such as glutamine and fatty acids are anaplerotic carbon sources in the TCA cycle that complicate these observations[9, 10]. Together these findings indicate that glycolysis can be gradually tuned with differing levels of intermediate metabolites.

The levels of cofactors and substrates that mediate protein acetylation are affected by glycolysis

Having demonstrated that gradually perturbing the rate of glycolysis results in gradual differences across metabolism, we then looked more closely at the metabolic network responsible for the levels of metabolites that mediate protein acetylation. Several metabolites related to glycolysis and others downstream of glucose metabolism that could affect acetylation were investigated. NAD^+ is the cofactor for sirtuins that carry out deacetylation reactions. It has also been postulated that sirtuins could be regulated by the NAD^+/NADH ratio. Beta-

Figure 2.2. 2DG treatment has a global effect on cellular metabolism.

(A) Heatmap of effects of 2DG treatment on global metabolism relative to Veh. (B) Effects of 2DG treatment on glycolytic metabolite levels relative to Veh. (C) Effects of 2DG treatment on TCA cycle intermediate levels relative to Veh. Mean ± SEM of triplicates

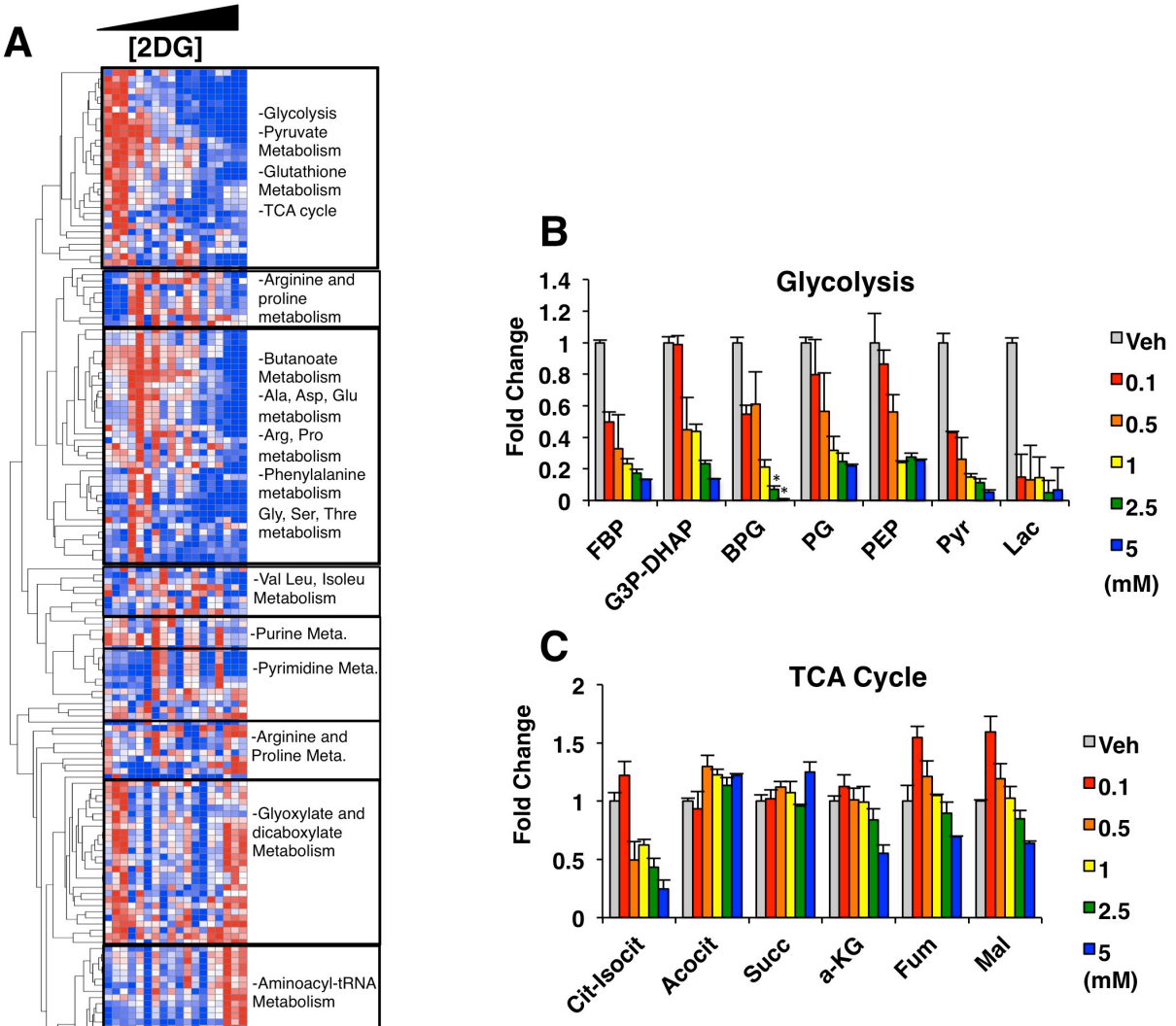
A
[2DG]
-Glycolysis
-Pyruvate Metabolism
-Glutathione Metabolism
-TCA cycle
-Arginine and proline metabolism
-Butanoate Metabolism
-Ala, Asp, Glu metabolism
-Arg, Pro metabolism
-Phenylalanine metabolism
Gly, Ser, Thre metabolism
-Val Leu, Isoleu Metabolism
-Purine Meta.
-Pyrimidine Meta.
-Arginine and Proline Meta.
-Glyoxylate and dicaboxylate Metabolism
-Aminoacyl-tRNA Metabolism
-Pentose Phosphate Metabolism
B
Glycolysis
Fold Change
1.4
1.2
1
0.8
0.6
0.4
0.2
0
FBP
G3P-DHAP
BPG
PG
PEP
Pyr
Lac
Veh
0.1
0.5
1
2.5
5
(mM)
C
TCA Cycle
Fold Change
2
1.5
1
0.5
0
Cit-Isocit
Acocit
Succ
a-KG
Fum
Mal
Veh
0.1
0.5
1
2.5
5
(mM)

hydroxybutryate (β-OHB), a ketone body, is a functional histone deacetylase (HDAC) inhibitor[30]. Also, both ac-CoA levels and the ratio of ac-CoA/CoA have been found to mediate acetylation reactions (Fig. 2.3A). Some of these results may be unexpected and differ from what has been reported in prior studies that have used manipulations such as glucose deprivation or calorie restriction[49]. These previous studies, however, have focused on long-term consequences of complete glycolytic inhibition as opposed to acute treatments that identify direct biochemical consequences.

We observed a dose-dependent gradual decrease of intracellular levels of ac-CoA (Fig. 2.3B) in response to 2DG treatment. We also observed a graded increase in the ac-CoA/CoA ratio (Fig. 2.3C). A smaller decrease in overall NAD^+ levels was also observed (Fig. 2.3D). The Pyr/Lac ratio, which is a surrogate for the cytosolic NAD^+/NADH ratio, decreased with 2DG treatment; however, this decrease was constant with all treatments (Fig. 2.3E). Both aceto-acetate, a ketone body, (Fig. 2.3F) and β-OHB (Fig. 2.3G) were unaffected by 2DG treatment. Together these results indicate that metabolites known to mediate protein acetylation via lysine acetyl transferases (KATs) are sensitive to glycolytic flux, whereas those known to be important for HDACs appear to be regulated by other fluxes.

Global histone acetylation levels are determined by glycolytic flux

Having observed a decrease in metabolites known to be involved in protein acetylation in response to 2DG, we next investigated whether there are corresponding changes in histone acetylation levels. We first considered whether histone acetylation would respond to glucose availability (Fig. 2.4A). We found, consistent with what has been previously described [21, 22, 49], histone acetylation levels were altered in response to changes in glucose availability. Indeed,

Figure 2.3. Glucose metabolism quantitatively alters substrates and co-factors for posttranslational modifications.

(A) Known metabolic pathways that can affect histone acetylation. (B) ac-CoA levels in response to 2DG treatments relative to Veh. (C) ac-CoA/CoA ratio in response to 2DG treatments relative to Veh. (D) NAD^+ levels in response to 2DG treatments relative to Veh. (E) Pyruvate/Lactate ratio in response to 2DG treatments relative to Veh. (F) ac-acetate levels in response to 2DG treatments relative to Veh. (G) β-hydroxybutyrate levels in response to 2DG treatments relative to Veh. Mean ± SEM of triplicates

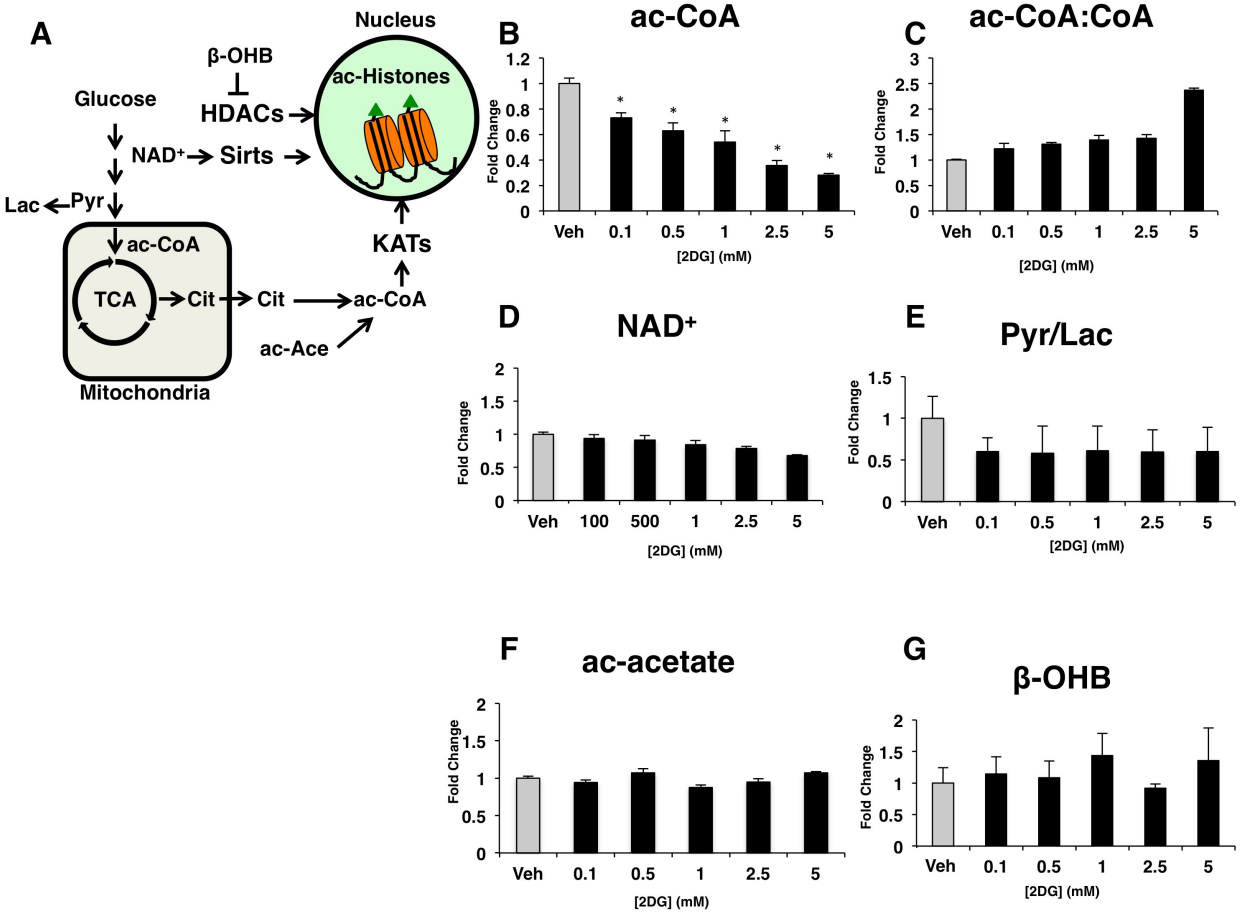
A
Nucleus
β-OHB
ac-Histones
Glucose
HDACs
NAD+
Sirts
Lac
Pyr
ac-CoA
KATs
TCA
Cit
Cit
ac-CoA
ac-Ace
Mitochondria
B
ac-CoA
Fold Change
Veh 0.1 0.5 1 2.5 5
[2DG] (mM)
C
ac-CoA:CoA
Fold Change
Veh 0.1 0.5 1 2.5 5
[2DG] (mM)
D
NAD+
Fold Change
Veh 100 500 1 2.5 5
[2DG] (mM)
E
Pyr/Lac
Fold Change
Veh 0.1 0.5 1 2.5 5
[2DG] (mM)
F
ac-acetate
Fold Change
Veh 0.1 0.5 1 2.5 5
[2DG] (mM)
G
β-OHB
Fold Change
Veh 0.1 0.5 1 2.5 5
[2DG] (mM)

we observe a dose dependent decrease of histone acetylation levels on global acetylated histone H3 (ac-H3) levels as well as acetylated histone H3 at residue 27 (H3K27) levels in response to 2DG treatments (Fig. 2.4B). These decreases had a strong positive correlation with ac-CoA (Fig. 2.4C), ac-CoA/CoA (Fig. 2.4D), Pyr/Lac (Fig. 4D) and NAD^+ levels (Fig. 2.4D). Together these results identify the variables in the metabolic network that are associated with ac-CoA and illustrate the precise metabolite levels that result from changes in glycolytic flux that are important for regulating histone acetylation levels.

Glycolytic flux can affect other histone acylation PTMs

We so far observed that changes in glycolytic flux induce corresponding changes in global acetylation levels and that there exists tight correlations with the levels of key metabolic variables and global histone acetylation levels. We next considered whether these changes occurred non-specifically across histones or whether specificity could be achieved through this mechanism as has been suggested.

To test this hypothesis, we performed a multiplexed stable isotopic labeling by amino acids in cell culture (SILAC) experiment. Such a procedure could determine quantitative changes of specific histone acetylation sites that were modulated by glucose. We cultured cells in three media conditions containing unlabeled (^{12}C) lysine (light), 4,4,5,5-D4-L-lysine (medium) and, $^{13}C_6{}^{15}N_2$-L-lysine (heavy). These conditions have been previously shown not to affect growth rate and are minimally metabolized in cells[50, 51]. We treated these SILAC-labeled cells with 0.1 mM (low), or 5mM (high) 2DG and compared them to DMSO (Veh) treated cells

Figure 2.4. The rate of glycolysis determines histone acetylation.

(A) Western Blot of Pan-acetyl-H3 and H3K27ac in response to glucose titration with quantification; total H3 was used as loading control. (B) Western Blot of Pan-acetyl-H3 and H3K27ac in response to 2DG treatment with quantification; total H3 was used as loading control. (C) Scatter-plot depicting correlation between ac-CoA levels and H3K27ac levels. (D) Bar graph of Spearman correlation coefficient of ac-CoA:CoA, β-OHB, ac-acetate, ac-CoA, CoA, Pyr/Lac and NAD^+. Mean ± SEM of triplicates (*P <0.05 versus Veh)

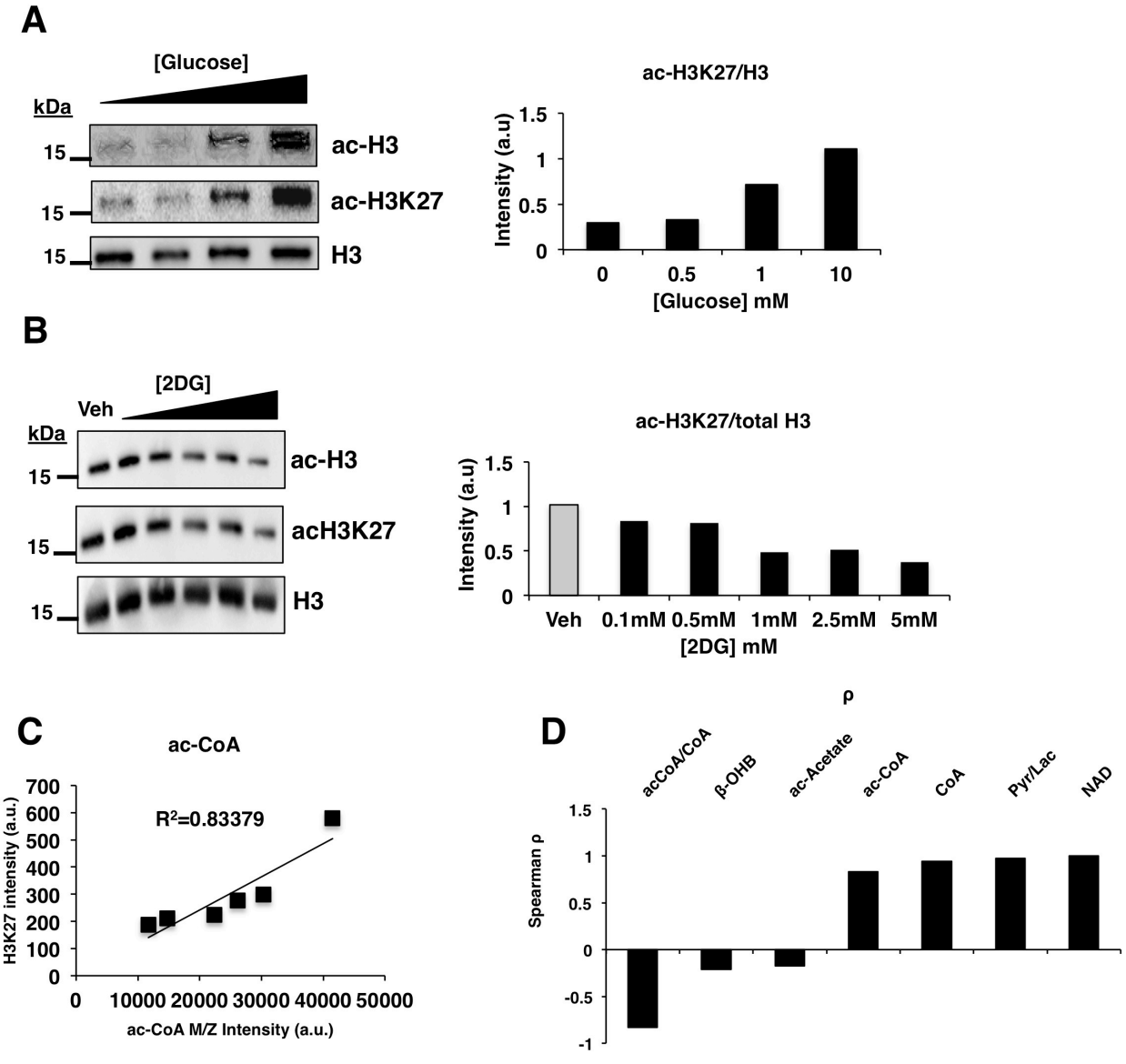
A
[Glucose]
kDa
15
ac-H3
15
ac-H3K27
15
H3
ac-H3K27/H3
Intensity (a.u)
1.5
1
0.5
0
0
0.5
1
10
[Glucose] mM
B
[2DG]
Veh
kDa
15
ac-H3
15
acH3K27
15
H3
ac-H3K27/total H3
Intensity (a.u)
1.5
1
0.5
0
Veh
0.1mM
0.5mM
1mM
2.5mM
5mM
[2DG] mM
C
ac-CoA
R²=0.83379
H3K27 intensity (a.u.)
700
600
500
400
300
200
100
0
0
10000
20000
30000
40000
50000
ac-CoA M/Z Intensity (a.u.)
D
ρ
acCoA/CoA
β-OHB
ac-Acetate
ac-CoA
CoA
Pyr/Lac
NAD
Spearman ρ
1.5
1
0.5
0
-0.5
-1

(Figure 2.5A). We identified a total of 17 acetylation sites on histones and after hierarchical clustering; distinct patterns of response were observed (Fig. 2.5B). Some residues exhibited no obvious trend in histone acetylation in response to changing rates of glycolytic flux. Others exhibited no change in total acetylation level. However, 7 identified acetylation sites exhibited a graded decrease in total levels in response to a decrease in glycolytic flux. Histone residues that exhibited this pattern included H3K9ac, H3K14ac, H3K18ac, H4K8ac, H4K12ac, and H4K16ac (Fig. 2.5B). After quantifying the differences in the change in acetylation across the three different rates of glycolysis, it was found that the levels of about 40 percent (7/17) of the acetylation sites changed in a gradual quantitative manner in response to a change in glycolysis (Fig. 2.5C). Moreover, these sites were highly correlated to both ac-CoA levels and ac-CoA/CoA ratios (Fig 2.5D). Together these data show that manipulating metabolic flux using 2DG treatments can have specific effects on individual histone acetylation marks and that these effects can be seen at low doses. In addition to acetylation, it has recently come to our attention that other lysine acylation modifications occur on histones. These modifications, rather than using ac-CoA as the substrate, use more chemically elaborate acyl-CoA metabolites as substrates and are derived from other parts of intermediary metabolism[52]. Whether they respond to glycolysis flux is not known. We therefore considered a further investigation of the extent that glycolysis may mediate the levels of other lysine residues. Using the previously developed multiplexed SILAC approach, we considered three additional histone lysine modifications, 2-hydroxyisobutyrylation (K_{hib}) (Fig. 2.6A), butyrylation (K_{bu}) (Fig. 6B), and propionylation (K_{pr}) (Fig. 2.6C) totaling an additional 32 histone modifications. We found that histone propionylation (K_{pr}) (Fig. 2.6C), histone butyrylation (K_{bu}) (Fig. 2.6B), and histone 2-hydroxyisobutyrylation

Figure 2.5. Quantitative proteomics identifies specific dose-dependent changes in histone acetylation.

(A) Schematic of SILAC experiment workflow. (B) Heatmap of all detected histone acetylated residues in response to 2DG treatment. (C) Correlation coefficients of acetylated histones in relation to CoA and ac-CoA levels. (D) Quantification of the difference in sensitivity of ac-Histone residues to 2DG treatment.

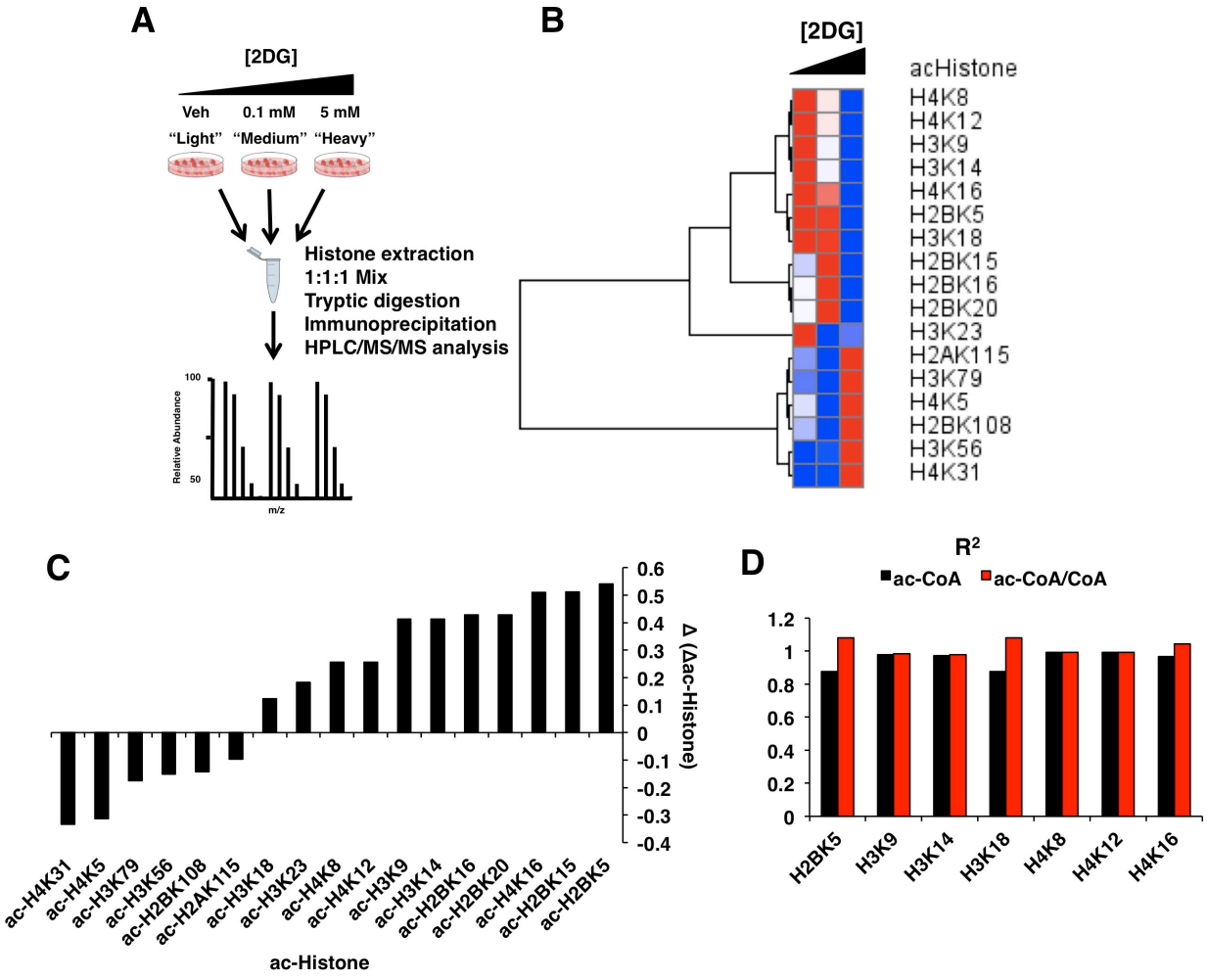
A
[2DG]
Veh
0.1 mM
5 mM
"Light"
"Medium"
"Heavy"
Histone extraction
1:1:1 Mix
Tryptic digestion
Immunoprecipitation
HPLC/MS/MS analysis
Relative Abundance
m/z
B
[2DG]
acHistone
H4K8
H4K12
H3K9
H3K14
H4K16
H2BK5
H3K18
H2BK15
H2BK16
H2BK20
H3K23
H2AK115
H3K79
H4K5
H2BK108
H3K56
H4K31
C
Δ (Δac-Histone)
ac-H4K31
ac-H4K5
ac-H3K79
ac-H3K56
ac-H2BK108
ac-H2AK115
ac-H3K18
ac-H3K23
ac-H4K8
ac-H4K12
ac-H3K9
ac-H3K14
ac-H2BK16
ac-H2BK20
ac-H4K16
ac-H2BK15
ac-H2BK5
ac-Histone
D
R²
ac-CoA
ac-CoA/CoA
H2BK5
H3K9
H3K14
H3K18
H4K8
H4K12
H4K16

(K_{hib}) (Fig. 2.6A) levels at all residues were gradually sensitive to glycolytic rate. Unlike lysine acetylation (K_{ac}), each of these modifications appeared to quantitatively respond to changes in glycolytic flux. Together these findings provide evidence that histone acylation exhibits specificity in response to changes in glycolytic rate.

Discussion

The molecular links between the metabolic state of cells and the status of protein acetylation have been intriguing [19, 20, 26, 53]. However, the direct quantitative biochemical interactions between metabolic flux, metabolite levels, and levels of protein acetylation have yet to be demonstrated. By considering a system that allows for controllable rates of glycolysis, this study resulted in a systematic analysis of factors in metabolism that contribute, with specificity, to acetylation levels. By considering histone modifications, this allowed for considerations of possible links between the metabolic state and cellular epigenetics. We were able to show that changes in glycolytic flux can have quantitative effects on global histone acetylation levels. This occurred first through changes in glycolytic rate having effects on the levels of metabolites in glycolysis and peripheral metabolism. Of all metabolites considered, ac-CoA and the ratio of ac-CoA to CoA appeared to have the strongest influence on histone acetylation.

Because most KATs have similar binding affinities to both ac-CoA and CoA, it has been suggested that the ac-CoA/CoA ratio may affect KAT activity as CoA can also have an inhibitory effect on some KATs[28]. Our findings demonstrate that decreasing glycolytic flux can decrease both ac-CoA and free CoA pools and that the regulation of these two pools are directly downstream of glycolysis. More importantly, our data suggests that the supply of intracellular ac-CoA has a greater effect on histone acetylation than the inhibitory effect of free

Figure 2.6. Histone acylation marks are sensitive to the rate of glycolysis.

(A) 2-hydroxyisobutrylation at H2BK5 in response to 2DG treatment. (B) Detected Propionylated histone residues responses to 2DG treatment. (C) Detected Butrylated histone residues responses to 2DG treatment. L:Light (Veh), M:Medium (0.1 mM 2DG), H:Heavy (5mM 2DG). The experiments described above were done by Ahmad Cluntun and He Huang.

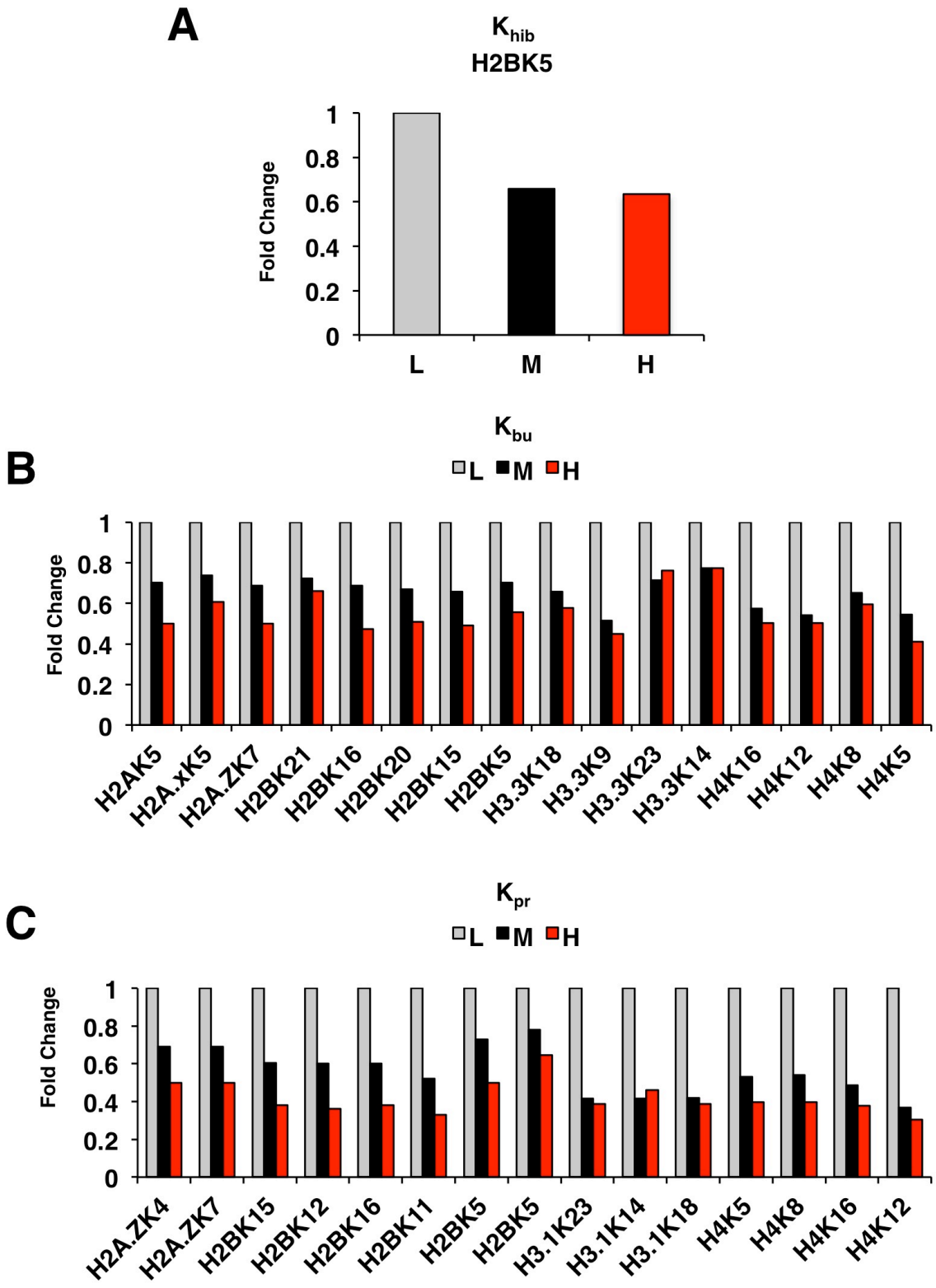
A
K_{hib}
H2BK5
Fold Change
1
0.8
0.6
0.4
0.2
0
L
M
H
B
K_{bu}
L M H
Fold Change
H2AK5
H2A.xK5
H2A.ZK7
H2BK21
H2BK16
H2BK20
H2BK15
H2BK5
H3.3K18
H3.3K9
H3.3K23
H3.3K14
H4K16
H4K12
H4K8
H4K5
C
K_{pr}
L M H
Fold Change
H2A.ZK4
H2A.ZK7
H2BK15
H2BK12
H2BK16
H2BK11
H2BK5
H2BK5
H3.1K23
H3.1K14
H3.1K18
H4K5
H4K8
H4K16
H4K12

CoA. Recently, it has been shown that the selectivity of p300, a histone acetyltransferase, can be manipulated by intracellular levels of ac-CoA[54]. Furthermore, work in yeast has shown that Gcn5 is important in mediating histone acetylation and is very sensitive to intracellular ac-CoA levels as well[19]. Our findings show that many other residues not known to be catalyzed by these enzymes are also sensitive to the ac-CoA levels suggesting that such a phenomenon is likely pervasive in cells. Interestingly, it has not escaped our attention that modifications located close to, or on globular histone domains seem to be more resistant to changes in glycolytic flux, whereas those on histone tails seem to be more sensitive suggesting that spatial proximity to the metabolic milieu may dictate in part those histone mark that are more dynamic. Moreover, we show that other histone acylation modifications are sensitive to glycolytic flux that likely follow similar principles.

Finally, histone Kac, Kpr, Kbu and Khib each appear to be globally regulated by glycolytic rate and have all been associated with active gene expression. It has been shown that these PTMs utilize corresponding acyl-CoA intermediates. However, it is not known they are all connected to glycolysis. From our data we can speculate that the decrease in free CoA restricts the ability to form the corresponding acyl-CoAs necessary for these PTMs suggesting some possibility of enzymatic activity mediating these reactions. The sensitivity of these PTMs to glycolytic flux is unexpected and further investigation is required that includes better understanding the chemical reaction mechanisms that mediate these PTMs. Their sensitivity to glycolytic flux may add to the increasing evolutionary benefits cancer cells gain from the Warburg effect as glycolytic rates are increased in these cells by as much as 200 fold compared to normal cells. An exciting recent study has demonstrated that resistance to targeted therapy can be driven by elevated nutrient levels[55]. As abnormal metabolism is a recurrent theme in

cancer, understanding its effect on chromatin biology may lead to newfound insights into tumor cell biology and the interaction between metabolism and gene regulation.

Conclusions

Multiple functions of the Warburg effect or the enhanced rate of glycolysis observed in tumors and proliferative tissue have been proposed. The most notable function in recent years is that the Warburg effect allows for increased biosynthesis [1,8]. This current study provides evidence for a new, lesser-appreciated interpretation of the Warburg Effect in that it confers direct signaling functions to cells by altering the levels of multiple key metabolites that serve as cofactors and substrates for reactions involving important post-translational modifications, notably histone acetylation, histone butyrylation, histone propionylation and histone 2-hydroxyisobutryrylation.

References

1. Pearce, E.L., et al., *Fueling immunity: insights into metabolism and lymphocyte function.* Science, 2013. **342**(6155): p. 1242454.
2. Ward, P.S. and C.B. Thompson, *Metabolic reprogramming: a cancer hallmark even warburg did not anticipate.* Cancer Cell, 2012. **21**(3): p. 297-308.
3. Koppenol, W.H., P.L. Bounds, and C.V. Dang, *Otto Warburg's contributions to current concepts of cancer metabolism.* Nat Rev Cancer, 2011. **11**(5): p. 325-37.
4. Locasale, J.W. and L.C. Cantley, *Metabolic flux and the regulation of mammalian cell growth.* Cell Metab, 2011. **14**(4): p. 443-51.
5. Locasale, J.W., *The consequences of enhanced cell-autonomous glucose metabolism.* Trends Endocrinol Metab, 2012. **23**(11): p. 545-51.
6. Epstein, T., et al., *Separation of metabolic supply and demand: aerobic glycolysis as a normal physiological response to fluctuating energetic demands in the membrane.* Cancer Metab, 2014. **2**: p. 7.
7. Pfeiffer, T., S. Schuster, and S. Bonhoeffer, *Cooperation and competition in the evolution of ATP-producing pathways.* Science, 2001. **292**(5516): p. 504-7.
8. Slavov, N., et al., *Constant growth rate can be supported by decreasing energy flux and increasing aerobic glycolysis.* Cell Rep, 2014. **7**(3): p. 705-14.
9. DeBerardinis, R.J., et al., *The biology of cancer: metabolic reprogramming fuels cell growth and proliferation.* Cell Metab, 2008. **7**(1): p. 11-20.
10. DeBerardinis, R.J., et al., *Beyond aerobic glycolysis: transformed cells can engage in glutamine metabolism that exceeds the requirement for protein and nucleotide synthesis.* Proc Natl Acad Sci U S A, 2007. **104**(49): p. 19345-50.

11. Dzeja, P.P. and A. Terzic, *Phosphotransfer networks and cellular energetics.* J Exp Biol, 2003. **206**(Pt 12): p. 2039-47.

12. Bittl, J.A. and J.S. Ingwall, *Reaction rates of creatine kinase and ATP synthesis in the isolated rat heart. A 31P NMR magnetization transfer study.* J Biol Chem, 1985. **260**(6): p. 3512-7.

13. Chang, C.H., et al., *Posttranscriptional control of T cell effector function by aerobic glycolysis.* Cell, 2013. **153**(6): p. 1239-51.

14. Slavov, N. and D. Botstein, *Decoupling nutrient signaling from growth rate causes aerobic glycolysis and deregulation of cell size and gene expression.* Mol Biol Cell, 2013. **24**(2): p. 157-68.

15. Gut, P. and E. Verdin, *The nexus of chromatin regulation and intermediary metabolism.* Nature, 2013. **502**(7472): p. 489-98.

16. Yun, J., et al., *Interactions between epigenetics and metabolism in cancers.* Front Oncol, 2012. **2**: p. 163.

17. Katada, S., A. Imhof, and P. Sassone-Corsi, *Connecting threads: epigenetics and metabolism.* Cell, 2012. **148**(1-2): p. 24-8.

18. Lu, C. and C.B. Thompson, *Metabolic regulation of epigenetics.* Cell Metab, 2012. **16**(1): p. 9-17.

19. Cai, L., et al., *Acetyl-CoA induces cell growth and proliferation by promoting the acetylation of histones at growth genes.* Mol Cell, 2011. **42**(4): p. 426-37.

20. Evertts, A.G., et al., *Quantitative dynamics of the link between cellular metabolism and histone acetylation.* J Biol Chem, 2013. **288**(17): p. 12142-51.

21. Moussaieff, A., et al., *Glycolysis-Mediated Changes in Acetyl-CoA and Histone*

Acetylation Control the Early Differentiation of Embryonic Stem Cells. Cell Metab, 2015. **21**(3): p. 392-402.

22. Liu, X.S., J.B. Little, and Z.M. Yuan, *Glycolytic metabolism influences global chromatin structure.* Oncotarget, 2015. **6**(6): p. 4214-25.
23. Takahashi, H., et al., *Nucleocytosolic acetyl-coenzyme a synthetase is required for histone acetylation and global transcription.* Mol Cell, 2006. **23**(2): p. 207-17.
24. Donohoe, D.R., et al., *The Warburg effect dictates the mechanism of butyrate-mediated histone acetylation and cell proliferation.* Mol Cell, 2012. **48**(4): p. 612-26.
25. Sutendra, G., et al., *A nuclear pyruvate dehydrogenase complex is important for the generation of acetyl-CoA and histone acetylation.* Cell, 2014. **158**(1): p. 84-97.
26. Wellen, K.E., et al., *ATP-citrate lyase links cellular metabolism to histone acetylation.* Science, 2009. **324**(5930): p. 1076-80.
27. McBrian, M.A., et al., *Histone acetylation regulates intracellular pH.* Mol Cell, 2013. **49**(2): p. 310-21.
28. Albaugh, B.N., K.M. Arnold, and J.M. Denu, *KAT(ching) metabolism by the tail: insight into the links between lysine acetyltransferases and metabolism.* Chembiochem, 2011. **12**(2): p. 290-8.
29. Finkel, T., C.X. Deng, and R. Mostoslavsky, *Recent progress in the biology and physiology of sirtuins.* Nature, 2009. **460**(7255): p. 587-91.
30. Shimazu, T., et al., *Suppression of oxidative stress by beta-hydroxybutyrate, an endogenous histone deacetylase inhibitor.* Science, 2013. **339**(6116): p. 211-4.
31. Huang, H., et al., *SnapShot: histone modifications.* Cell, 2014. **159**(2): p. 458-458 e1.
32. Dai, L., et al., *Lysine 2-hydroxyisobutyrylation is a widely distributed active histone*

mark. Nat Chem Biol, 2014. **10**(5): p. 365-70.

33. Tan, M., et al., *Identification of 67 histone marks and histone lysine crotonylation as a new type of histone modification.* Cell, 2011. **146**(6): p. 1016-28.

34. Chen, Y., et al., *Lysine propionylation and butyrylation are novel post-translational modifications in histones.* Mol Cell Proteomics, 2007. **6**(5): p. 812-9.

35. Liu, X., et al., *A strategy for sensitive, large scale quantitative metabolomics.* J Vis Exp, 2014(87).

36. Liu, X., Z. Ser, and J.W. Locasale, *Development and quantitative evaluation of a high-resolution metabolomics technology.* Anal Chem, 2014. **86**(4): p. 2175-84.

37. Shechter, D., et al., *Extraction, purification and analysis of histones.* Nat Protoc, 2007. **2**(6): p. 1445-57.

38. Cox, J. and M. Mann, *MaxQuant enables high peptide identification rates, individualized p.p.b.-range mass accuracies and proteome-wide protein quantification.* Nat Biotechnol, 2008. **26**(12): p. 1367-72.

39. Cox, J., et al., *Andromeda: a peptide search engine integrated into the MaxQuant environment.* J Proteome Res, 2011. **10**(4): p. 1794-805.

40. Wick, A.N., et al., *Localization of the primary metabolic block produced by 2-deoxyglucose.* J Biol Chem, 1957. **224**(2): p. 963-9.

41. Brown, J., *Effects of 2-deoxyglucose on carbohydrate metablism: review of the literature and studies in the rat.* Metabolism, 1962. **11**: p. 1098-112.

42. Sols, A. and R.K. Crane, *Substrate specificity of brain hexokinase.* J Biol Chem, 1954. **210**(2): p. 581-95.

43. Nirenberg, M.W. and J.F. Hogg, *Inhibition of anaerobic glycolysis in Ehrlich ascites*

tumor cells by 2-deoxy-D-glucose. Cancer Res, 1958. **18**(5): p. 518-21.

44. Chen, W. and M. Gueron, *The inhibition of bovine heart hexokinase by 2-deoxy-D-glucose-6-phosphate: characterization by 31P NMR and metabolic implications.* Biochimie, 1992. **74**(9-10): p. 867-73.

45. Kurtoglu, M., J.C. Maher, and T.J. Lampidis, *Differential toxic mechanisms of 2-deoxy-D-glucose versus 2-fluorodeoxy-D-glucose in hypoxic and normoxic tumor cells.* Antioxid Redox Signal, 2007. **9**(9): p. 1383-90.

46. Vander Heiden, M.G., *Targeting cancer metabolism: a therapeutic window opens.* Nat Rev Drug Discov, 2011. **10**(9): p. 671-84.

47. Xi, H., M. Kurtoglu, and T.J. Lampidis, *The wonders of 2-deoxy-D-glucose.* IUBMB Life, 2014. **66**(2): p. 110-21.

48. Ser, Z., et al., *Extraction parameters for metabolomics from cultured cells.* Anal Biochem, 2015. **475**: p. 22-8.

49. Lee, J.V., et al., *Akt-dependent metabolic reprogramming regulates tumor cell histone acetylation.* Cell Metab, 2014. **20**(2): p. 306-19.

50. Mann, M., *Functional and quantitative proteomics using SILAC.* Nat Rev Mol Cell Biol, 2006. **7**(12): p. 952-8.

51. Ong, S.E. and M. Mann, *A practical recipe for stable isotope labeling by amino acids in cell culture (SILAC).* Nat Protoc, 2006. **1**(6): p. 2650-60.

52. Sabari, B.R., et al., *Metabolic regulation of gene expression through histone acylations.* Nat Rev Mol Cell Biol, 2017. **18**(2): p. 90-101.

53. Zheng, Y., P.M. Thomas, and N.L. Kelleher, *Measurement of acetylation turnover at distinct lysines in human histones identifies long-lived acetylation sites.* Nat Commun,

2013. **4**: p. 2203.

54. Henry, R.A., et al., *Changing the Selectivity of p300 by Acetyl-CoA Modulation of Histone Acetylation.* ACS Chem Biol, 2014.

55. Masui, K., et al., *Glucose-dependent acetylation of Rictor promotes targeted cancer therapy resistance.* Proc Natl Acad Sci U S A, 2015.

Chapter 3

[‡]Defining the role of the glutaminase isozyme GLS2 in breast cancer cells

Abstract

Breast cancer is a heterogeneous disease that can be divided into five subtypes, each of which have been shown to be metabolically distinct. This includes differences in glutamine dependency between these subtypes. Two genes, GLS and GLS2, code the glutaminase enzyme in mammals. Although, the GLS enzyme has been intensely characterized, the GLS2 enzyme remains poorly studied. In this chapter, we identify GLS2 as a critical, metabolically active enzyme in breast cancer cells, and establish that GLS2 can mediate TCA cycle anaplerosis in these cells. Moreover, we establish that breast cancer cell subtypes exhibit distinct expression patterns of these two glutaminase enzymes. The small molecule, 968, is an effective inhibitor of both GLS and GLS2. We show that treating breast cancer cells with this inhibitor, can decrease ^{13}C-glutamine labeling of TCA cycle intermediates regardless of GLS or GLS2 expression levels. This sheds new light on the metabolic heterogeneity of breast cancer metabolism, and has important implications due to the fact that a glutaminase inhibitor, which fails to block GLS2 activity, is currently in Phase II trials.

[‡]This work was done in collaboration with Dr. Michael J. Lukey. Contributions: MJL and AAC designed the study, maintained the cell cultures and performed the drug treatment assays, MJL performed all the immunoblot assays and created all the knockdowns, AAC wrote this chapter, made all the figures, designed and performed all the metabolomics experiments, including running the metabolites on the HPLC/MS/MS, as well as collecting and analyzing the data and performed the 968 time course assay.

Introduction

Despite treatment advances, breast cancer remains a leading cause of cancer deaths among women worldwide[1]. This may be partially due to the fact that genomic studies have established breast cancer as a complex heterogeneous disease that can be divided into five intrinsic subtypes (Luminal A, Luminal B, HER2-enriched, Claudin-low, Basal-like) and a normal breast-like group[2, 3]. Recently, these subtypes have been shown to be metabolically distinct, as luminal breast cancer cells typically exhibit increased glucose uptake, whereas most basal breast cancer cells rapidly consume the amino acid glutamine[4].

Increased uptake of glutamine by cancer cells can help fulfill biosynthetic demands associated with proliferation[5], including the requirement for an anaplerotic pathway to maintain the tricarboxylic acid (TCA) cycle[6]. Glutamine is unique in its ability to serve as an important source of both carbon and nitrogen[6]. Consequently, there has been a growing interest in identifying targets to disrupt the ability of cancer cells to utilize this nutrient. One such target is the mitochondrial enzyme glutaminase (GLS), which converts glutamine to glutamate.

In mammalian cells, two genes encode glutaminase enzymes, *GLS* and *GLS2*. GLS has been intensely studied and currently has a selective inhibitor, CB-839, under evaluation in clinical trials for treatment of triple-negative breast cancer and renal cell carcinoma[7]. The GLS and GLS2 proteins are highly homologous, and most reports indicate that both are localized to mitochondria [8-10]. However, although it is well established that GLS is highly expressed and important for growth of several cancer types, there is less clarity on the role of GLS2 in tumorigenesis, since it has been reported to be downregulated in liver cancer and glioblastoma[11, 12], yet upregulated in neuroblastoma[13], colon cancer[14] and cervical cancer[15]. Here, we identify GLS2 as a critical metabolic enzyme in luminal breast cancer

cells, and establish that GLS2 mediates TCA cycle anaplerosis in this breast cancer subtype. We also demonstrate that the glutaminase inhibitor 968 is an effective inhibitor of both GLS and GLS2, in contrast to BPTES and CB-839 which selectively target the GLS isozyme. Moreover, we establish that breast cancer cell subtypes exhibit distinct expression patterns of the two glutaminase enzymes. This shed new light on the metabolic heterogeneity of breast cancer metabolism and may help guide future treatment strategies.

Results

GLS and GLS2 have distinct expression levels in luminal and basal breast cancer cells

We initially selected a panel of breast cancer cell lines with varying degrees of glutamine dependency, including luminal breast cancer-derived cell lines that can survive and proliferate, albeit at a decreased rate, in the absence of exogenous glutamine (T-47D and MCF7), a glutamine-dependent luminal breast cancer cell line (MDA-MB-453), and glutamine-dependent basal breast cancer-derived cell lines (Hs 578T, MDA-MB-231 and TSE) (Figure 3.1A). To confirm the breast cancer cell line subtypes, we performed an immunoblot analysis and used GATA binding protein 3 (GATA3) as a marker of luminal breast cancers. We also assessed levels of both glutaminase proteins, GLS and GLS2, in these cell lines (Figure 3.1A). All of the glutamine-dependent basal cell lines expressed high levels of GLS but very low or undetectable levels of GLS2. The luminal cells expressed lower levels of GLS and higher levels of GLS2, and MDA-MB-453 cells expressed GLS2 exclusively. Taken together, we confirm that basal and luminal breast cancer cell lines have unique GLS and GLS2 expression profiles.

Figure 3.1. Basal and luminal breast cancer cell lines have distinct glutaminase isozyme expression patterns.

A. Representative Western blots for GLS and GLS2 levels across a number of breast cancer cell lines. All samples were run on the same gel, reorganized here for presentation. B. Heatmap of hierarchical clustering of global metabolite levels across all cell lines (HS 578T not shown). GATA3: GATA binding protein 3, GLS2: glutaminase 2, GLS: glutaminase, 453: MDA-MB-453, 231: MDA-MB-231, Lum: Luminal breast cancer cells, Bas: Basal breast cancer cells.

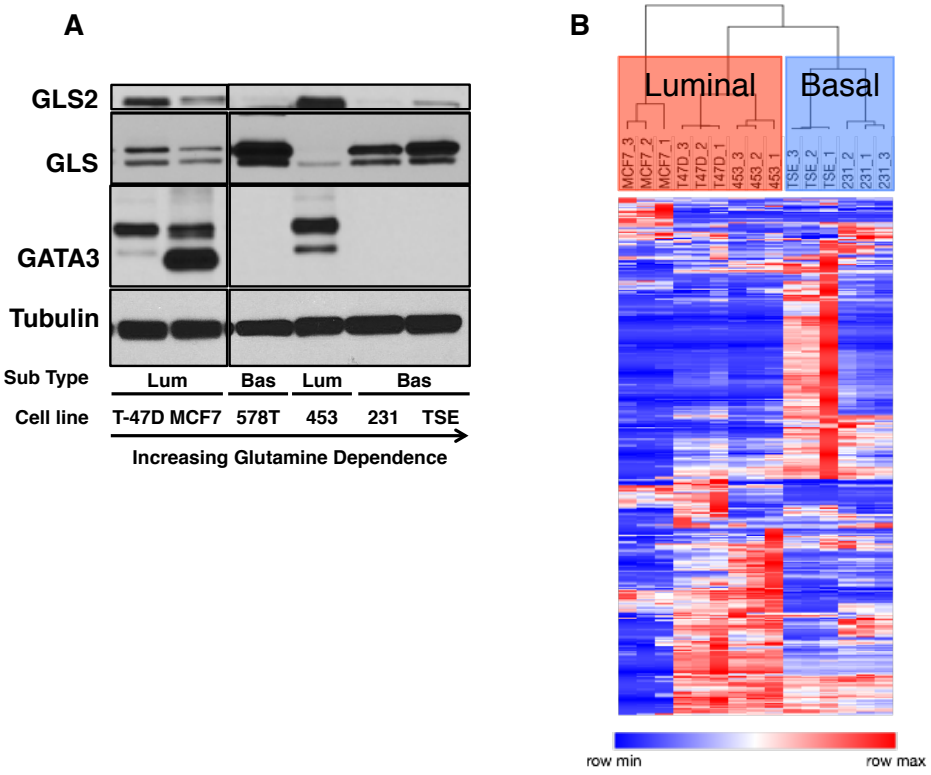
A
GLS2
GLS
GATA3
Tubulin
Sub Type
Lum
Bas
Lum
Bas
Cell line
T-47D MCF7
578T
453
231
TSE
Increasing Glutamine Dependence
B
Luminal
Basal
MCF7_3
MCF7_2
MCF7_1
T47D_3
T47D_2
T47D_1
453_3
453_2
453_1
TSE_3
TSE_2
TSE_1
231_2
231_1
231_3
row min
row max

Basal and luminal breast cancer cells cluster according to their metabolome

To investigate the differences between these cell lines in their global metabolic patterns, we generated a profile of global metabolites for each cell line using liquid chromatography coupled to high-resolution mass spectrometry (LC-MS). Remarkably, a hierarchical clustering of the metabolomics data across the cell lines clustered the cell lines into luminal and basal (Figure 3.1B). Moreover, each of these subtypes display an enrichment of various pathways related to glutamine metabolism (Table 4.1). These results confirm that luminal and basal breast cancer cells are metabolically distinct. Moreover, irrespective of their dependence on an abundant extracellular supply of glutamine, all of these cell lines are enriched in metabolites that are related to glutamine metabolism.

Glutamine metabolism can feed the TCA cycle in both basal and luminal breast cancer cells

Since both subtypes showed an enrichment of glutamine metabolism pathways, we next sought to investigate how these cells utilize glutamine. To this end, we performed a stable 13-C glutamine tracing experiment. We specifically targeted the TCA cycle intermediates to determine whether or not GLS2 can feed this critical pathway in a manner similar to GLS. Indeed, we find that glutamine was able to feed the TCA cycle across all cell lines (Figure 3.2B). This includes MDA-MB-453 cells, which exclusively express GLS2 and have no detectable levels of GLS. None of the cell lines utilized reductive carboxylation, as indicated by the lack of any M+5 isotopomers of citrate. However, cell lines were grown in normoxic, monolayer cell culture conditions, and it is possible that these patterns would be altered under hypoxia or in 3D culture conditions. Taken together, we show that breast cancer cell lines that express either GLS or GLS2 utilize glutamine metabolism to feed the TCA cycle.

Table 4.1. Enriched metabolic pathways according to breast cancer subtype.

Luminal Breast Cancer Cells	Basal Breast Cancer Cells
Fatty acid biosynthesis	Ala, Asp, Glu metabolism
L-Glutamine and L-glutamate metabolism	Gly, Ser, Thr metabolism
Purine metabolism	Aminoacyl-tRNA biosynthesis
Linoleic acid metabolism	Arg and Pro metabolism
Alanine, aspartate and glutamate metabolism	Val, Leu, Iso biosynthesis
Glycolysis or Gluconeogenesis	Nitrogen metabolism
Pyruvate metabolism	Arg, Orn metabolism

Glutaminase inhibition has variable effects on basal and luminal breast cancer cells

Having determined that glutamine is feeding the TCA cycle in each of the breast cancer cell lines, we next investigated the roles of GLS and GLS2. To achieve this, we treated the cell lines with two allosteric inhibitors of glutaminase, bis-2-(5- phenylacetamido-1,2,4-thiadiazol-2-yl)ethyl sulfide (BPTES) and the benzophenanthridone known as 968. BPTES is a GLS-specific inhibitor[16], whereas 968 can inhibit both GLS and GLS2[17-19]. We performed the experiments on cells growing in medium containing ^{13}C labeled glutamine. The inhibitors were added simultaneously with the labeled media and the cells were left to grow in this media for 10 hours (see methods of details). We then extracted metabolites from these cells and paid specific attention to the TCA cycle intermediates downstream of the glutaminase reaction. We observed a significant decrease in the labeling patterns of TCA cycle intermediates downstream of GLS in basal breast cancer cell lines in response to BPTES treatment, relative to the untreated vehicle cells (Figure 3.3B). We also observed variable degrees of resistance to BPTES treatment in the GLS2-expressing luminal breast cancer cell lines (Figure 3.4B). This can be attributed to the fact that some GLS is expressed in MCF7 and T-47D cells, in addition to GLS2. MDA-MB-453 cells, which do not express any GLS and have high levels of GLS2, showed complete resistance to the BPTES treatment (Figure 3.4B). It is important to note that all of these TCA cycle intermediates have cytosolic pools[10], moreover, there are multiple anaplerotic pathways that can supply the TCA cycle beyond glutamine metabolism that can account for the complexity and variability in the degree of sensitivity to these inhibitors[6]. After 10 hours treatment, 968 had very little effect on any of the cells compared to the vehicle, whereas BPTES treatment had a strong effect on cells that express GLS, but little to no effect on cells that expressed GLS2. Later in this chapter, we describe experiments designed to assess the effects of more prolonged

Figure 3.2. Glutamine can feed TCA cycle anaplerosis in both basal and luminal breast cancer cells.

A. Schematic depicting the incorporation of 13C from glutamine into the TCA cycle. B. Bar graphs depicting the abundance ratios of relevant isotopologue species of TCA cycle intermediates. Glu: glutamate, α-KG: alpha-ketoglutarate, Succ: succinate, Fum: fumarate, Mal: malate, Cit/Iso: citrate-isocitrate. Mean ± SEM of triplicates

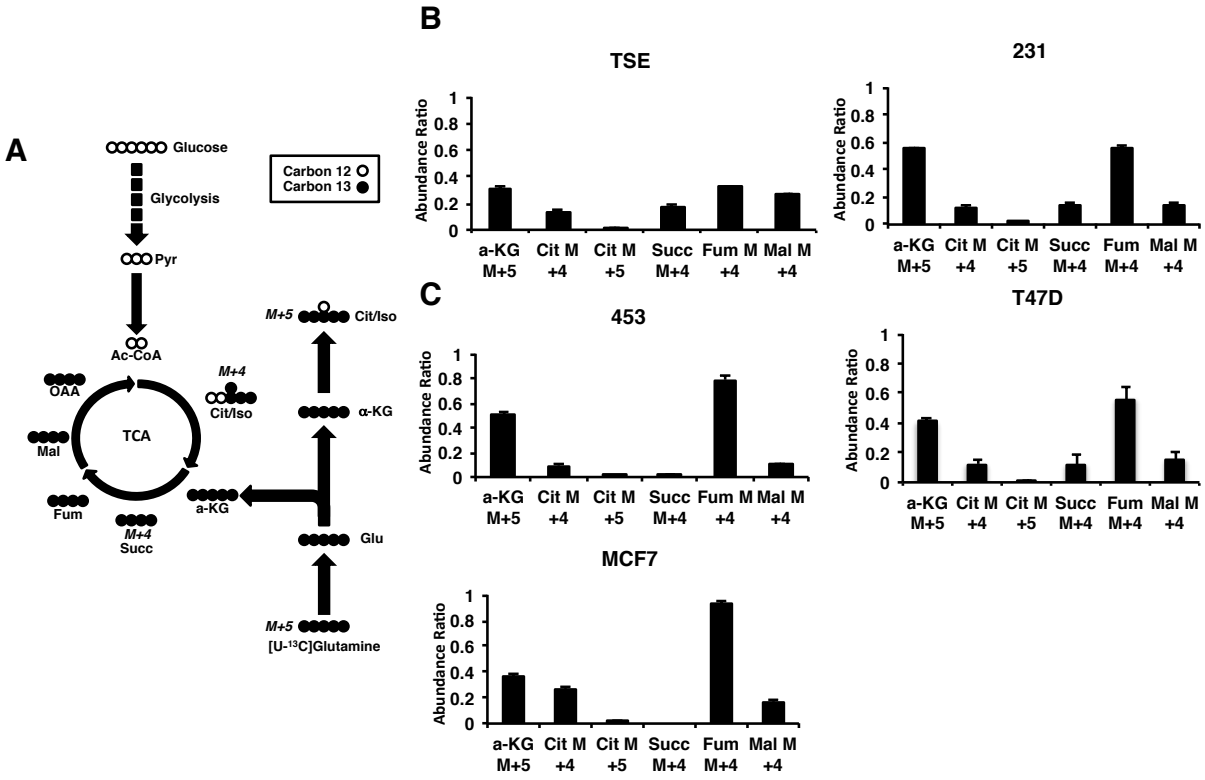
A
Glucose
Glycolysis
Pyr
Ac-CoA
OAA
TCA
Mal
Fum
Succ
Cit/Iso
α-KG
a-KG
Glu
M+5
M+4
[U-13C]Glutamine
Carbon 12
Carbon 13
B
TSE
231
C
453
T47D
MCF7
Abundance Ratio
a-KG M+5
Cit M +4
Cit M +5
Succ M+4
Fum M+4
Mal M +4

Figure 3.3. Effects of BPTES and 968 treatments on metabolites downstream of glutaminase in basal breast cancer cells.

A. Schematic depicting the incorporation of 13C from glutamine into the TCA cycle. B. Bar graphs depicting abundance ratios of relevant isotopologue species of TCA cycle intermediates in BPTES and 968 treated and untreated (vehicle) basal cells. Inhibitors were added at a final concentration of 10uM cultured in media containing labeled 13C-Glutmaine for 10 hours. 231: MDA-MB-231, Gln: glutamine, Glu: glutamate, α-KG: alpha-ketoglutarate, Succ: succinate, Fum: fumarate, Mal: malate, Cit/Iso: citrate-isocitrate. Mean ± SEM of triplicates

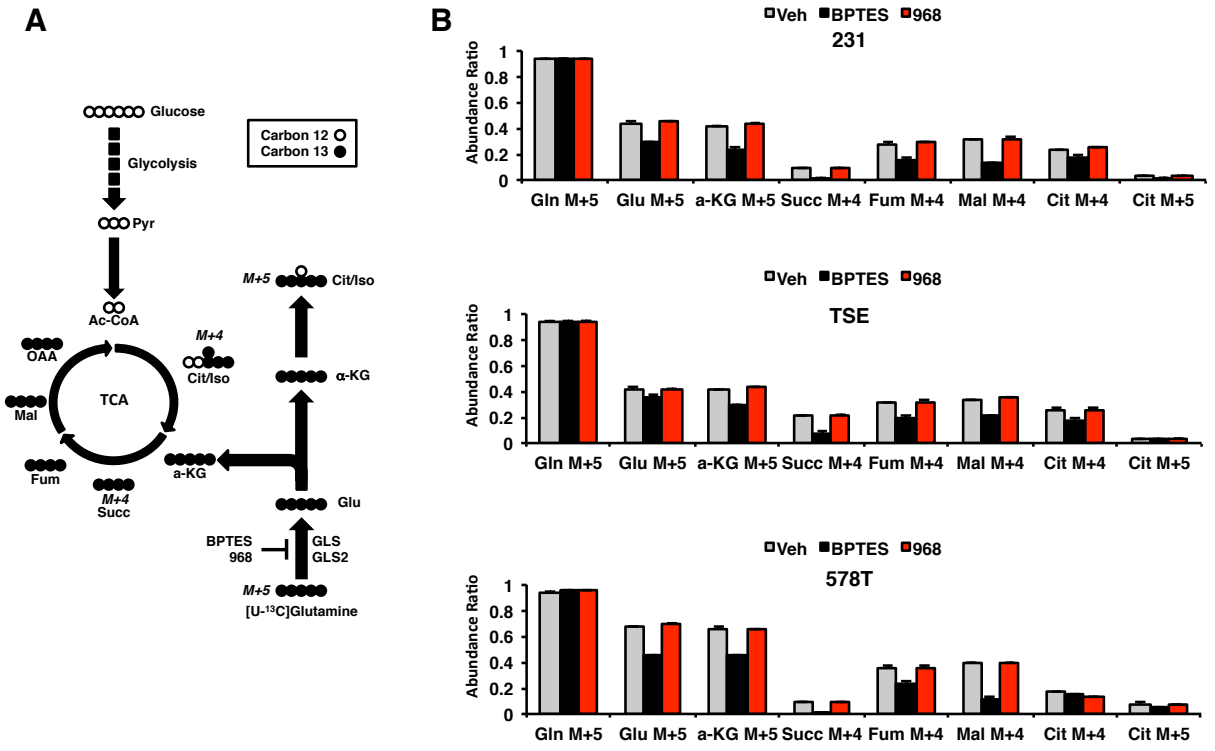
A
Glucose
Glycolysis
Pyr
Ac-CoA
OAA
TCA
Mal
Fum
M+4
Succ
M+4
Cit/Iso
a-KG
M+5
Cit/Iso
α-KG
Glu
BPTES
968
GLS
GLS2
M+5
[U-13C]Glutamine
Carbon 12
Carbon 13
B
Veh
BPTES
968
231
Abundance Ratio
1
0.8
0.6
0.4
0.2
0
Gln M+5
Glu M+5
a-KG M+5
Succ M+4
Fum M+4
Mal M+4
Cit M+4
Cit M+5
Veh
BPTES
968
TSE
Abundance Ratio
1
0.8
0.6
0.4
0.2
0
Gln M+5
Glu M+5
a-KG M+5
Succ M+4
Fum M+4
Mal M+4
Cit M+4
Cit M+5
Veh
BPTES
968
578T
Abundance Ratio
1
0.8
0.6
0.4
0.2
0
Gln M+5
Glu M+5
a-KG M+5
Succ M+4
Fum M+4
Mal M+4
Cit M+4
Cit M+5

Figure 3.4. Effects of BPTES and 968 treatments on metabolites downstream of glutaminase in luminal breast cancer cells.

A. Schematic depicting the incorporation of 13C from glutamine into the TCA cycle. B. Bar graphs depicting abundance ratios of relevant isotopologue species of TCA cycle intermediates in BPTES and 968 treated and untreated (vehicle) luminal cells. Inhibitors were added at a final concentration of 10uM cultured in media containing labeled 13C-Glutmaine for 10 hours. 453: MDA-MB-453, Gln: glutamine, Glu: glutamate, α-KG: alpha-ketoglutarate, Succ: succinate, Fum: fumarate, Mal: malate, Cit/Iso: citrate-isocitrate. Mean ± SEM of triplicates

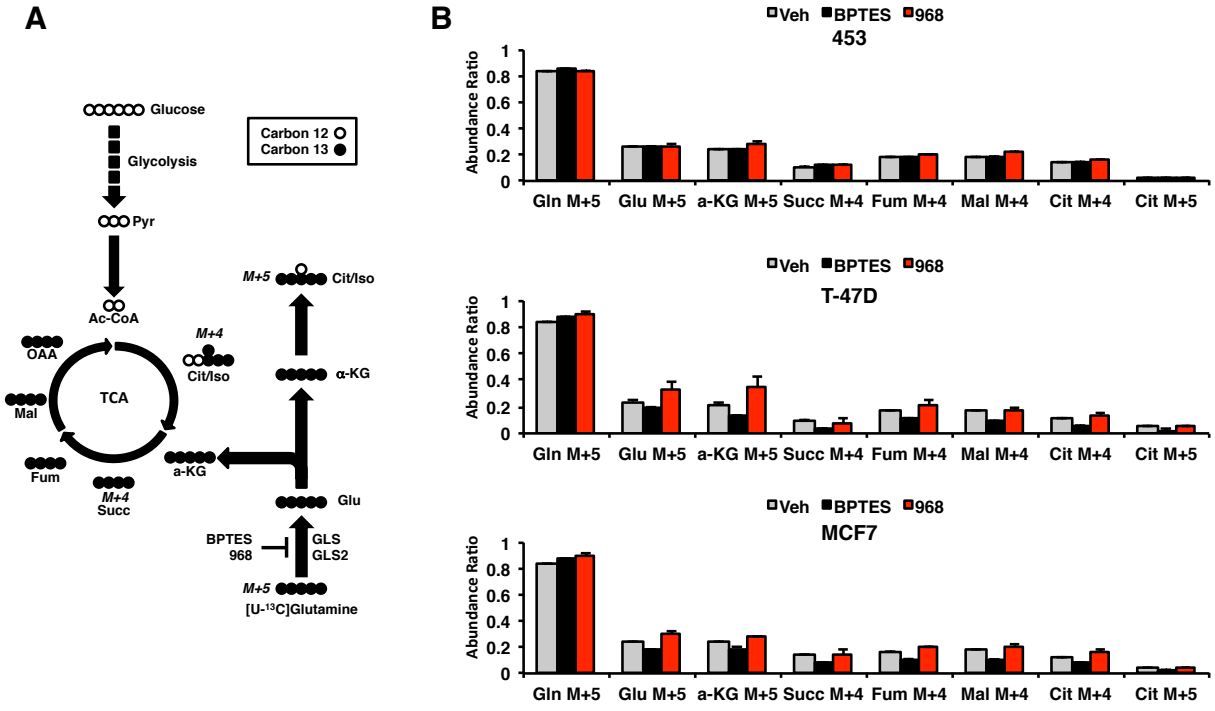
A
Glucose
Carbon 12
Carbon 13
Glycolysis
Pyr
Ac-CoA
OAA
TCA
Mal
Fum
M+4
Succ
M+4
Cit/Iso
M+5
Cit/Iso
α-KG
a-KG
Glu
BPTES
968
GLS
GLS2
M+5
[U-13C]Glutamine
B
Veh
BPTES
968
453
T-47D
MCF7
Abundance Ratio
0
0.2
0.4
0.6
0.8
1
Gln M+5
Glu M+5
a-KG M+5
Succ M+4
Fum M+4
Mal M+4
Cit M+4
Cit M+5

treatment with 968.

GLS2 is an important metabolic enzyme that can feed the TCA cycle

To investigate the roles of GLS and GLS in breast cancer cells, we next used genetic approaches to knockdown levels of these isozymes, and repeated the labeling experiment to detect changes in flux into the TCA cycle. We used short hairpin RNAs (shRNAs) to specifically target either GLS or GLS2. For both enzymes, we selected the two constructs that gave the most potent knockdown (Figure 3.5A, Figure 3.6A). In the basal breast cancer cell lines, MDA-MB-231 and TSE, knocking down GLS had a similar effect as BPTES treatment, with a decrease in labeling of TCA cycle intermediates observed (Figure 3.5C).

In the luminal breast cancer cell line MDA-MB-453, which exclusively expresses GLS2, knocking down GLS2 levels severely diminished the labeling of TCA cycle intermediates from glutamine (Figure 3.6C), thereby confirming GLS2 as a metabolically active enzyme. To our knowledge, this is the first report establishing GLS2 as an important enzyme for TCA cycle anaplerosis in breast cancer cells. Selective knockdowns of a single isozyme had the most potent effects in MDA-MB-231 (GLS) and MDA-MB453 (GLS2) cells, presumably because these cells express only one glutaminase isozyme, whereas TSE and T47D cells express both GLS and GLS2. Nevertheless, we do still detect decreases in the levels of glutamate, α-ketoglutarate and succinate, indicating that it is likely that these cells use both isozymes to varying degrees.

968 can inhibit both GLS and GLS2

To further investigate the impact of 968 treatment, we exposed cells to 968 for longer incubation times. Previous studies have shown that 968 preferentially binds to monomeric glutaminase[17],

Figure 3.5. Effects of knocking down GLS on metabolites downstream of glutaminase in basal breast cancer cells.

A. Immunoblot depicting the efficacy of the five shRNA constructs in knocking down levels of GLS, 48 hours after viral transduction. B. Schematic depicting the incorporation of ^{13}C from glutamine into the TCA cycle. C. Bar graphs depicting abundance ratios of relevant isotopologue species of TCA cycle intermediates in control shRNA and GLS-targeted shRNA transduced basal breast cancer cells cultured in media containing labeled ^{13}C-Glutmaine for 10 hours. 231: MDA-MB-231, Gln: glutamine, Glu: glutamate, α-KG: alpha-ketoglutarate, Succ: succinate, Fum: fumarate, Mal: malate, Cit-Iso: citrate-isocitrate. Mean ± SEM of triplicates

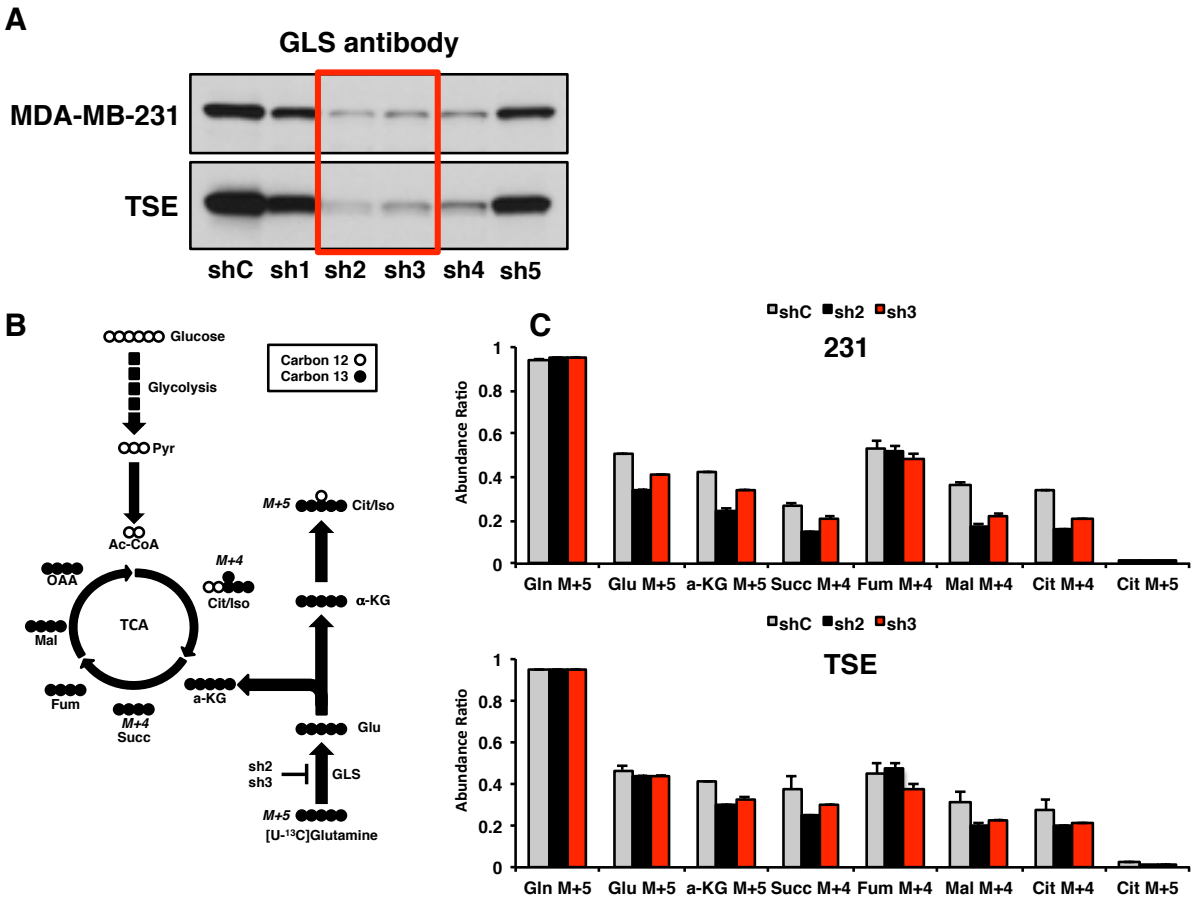
A
GLS antibody
MDA-MB-231
TSE
shC sh1 sh2 sh3 sh4 sh5
B
Glucose
Glycolysis
Pyr
Ac-CoA
OAA
TCA
Mal
Fum
M+4
Succ
M+4
Cit/Iso
a-KG
M+5
Cit/Iso
α-KG
Glu
sh2
sh3
GLS
M+5
[U-13C]Glutamine
Carbon 12
Carbon 13
C
shC sh2 sh3
231
Abundance Ratio
1
0.8
0.6
0.4
0.2
0
Gln M+5
Glu M+5
a-KG M+5
Succ M+4
Fum M+4
Mal M+4
Cit M+4
Cit M+5
shC sh2 sh3
TSE
Abundance Ratio
1
0.8
0.6
0.4
0.2
0
Gln M+5
Glu M+5
a-KG M+5
Succ M+4
Fum M+4
Mal M+4
Cit M+4
Cit M+5

Figure 3.6. Effects of knocking down GLS2 on metabolites downstream of glutaminase in luminal breast cancer cells.

A. Immunoblot depicting the efficacy of the five shRNA constructs in knocking down GLS2 levels, 48 hours after viral transduction. B. Schematic depicting the incorporation of ^{13}C from glutamine into the TCA cycle. C. Bar graphs depicting abundance ratios of relevant isotopologue species of TCA cycle intermediates in control shRNA and GLS2-targeted shRNA-transduced luminal breast cancer cells cultured in media containing labeled ^{13}C-Glutmaine for 10 hours. 453: MDA-MB-453, Gln: glutamine, Glu: glutamate, α-KG: alpha-ketoglutarate, Succ: succinate, Fum: fumarate, Mal: malate, Cit-Iso: citrate-isocitrate. Mean ± SEM of triplicates

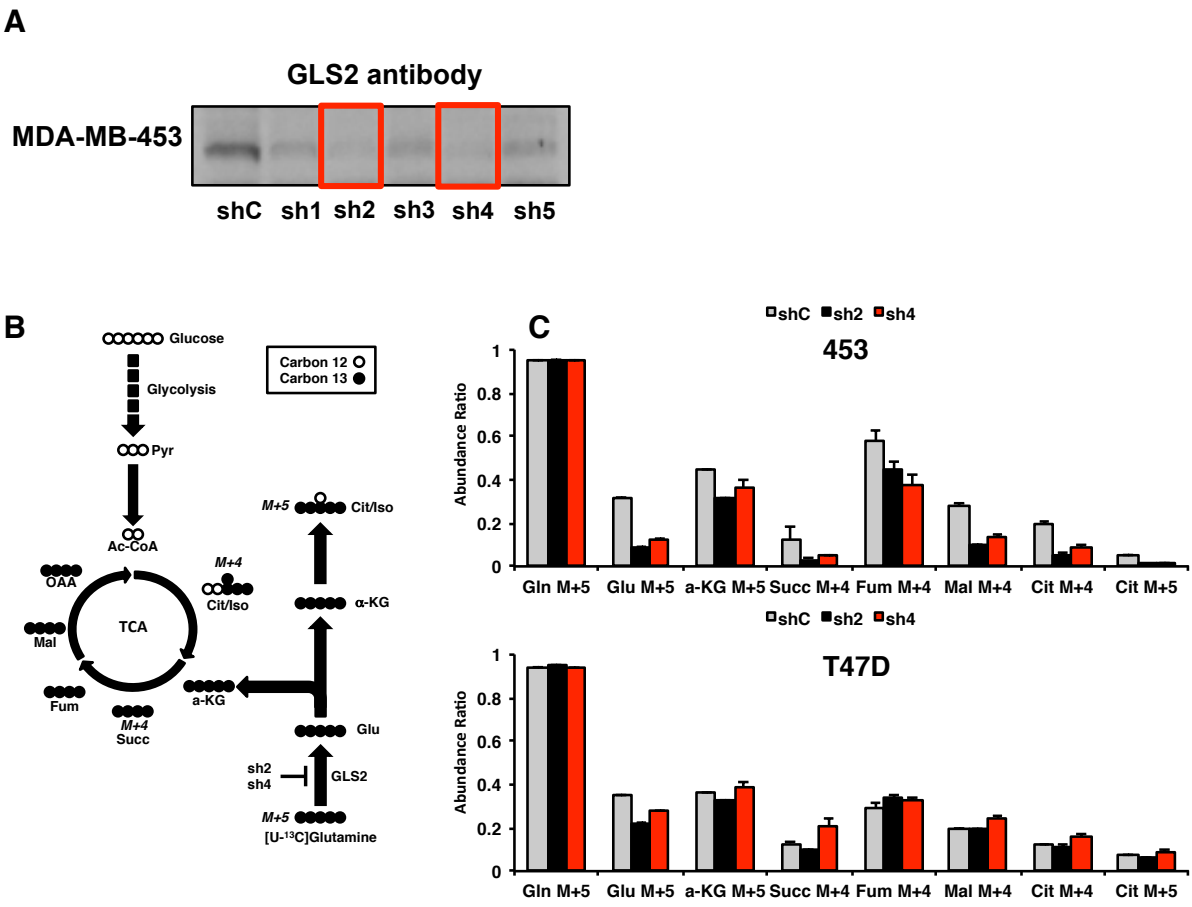
A
GLS2 antibody
MDA-MB-453
shC sh1 sh2 sh3 sh4 sh5
B
Glucose
Glycolysis
Pyr
Ac-CoA
OAA
TCA
Mal
Fum
M+4
Succ
M+4
Cit/Iso
M+5
Cit/Iso
α-KG
a-KG
Glu
sh2
sh4
GLS2
M+5
[U-13C]Glutamine
Carbon 12
Carbon 13
C
shC sh2 sh4
453
Abundance Ratio
Gln M+5 Glu M+5 a-KG M+5 Succ M+4 Fum M+4 Mal M+4 Cit M+4 Cit M+5
shC sh2 sh4
T47D
Abundance Ratio
Gln M+5 Glu M+5 a-KG M+5 Succ M+4 Fum M+4 Mal M+4 Cit M+4 Cit M+5

Figure 3.7. 968 requires extended incubation times to inhibit GLS2 in MDA-MB-453 cells.

Bar graphs depicting relative abundance of relevant TCA cycle intermediates in 968-treated MDA-MB-453 cells compared to the untreated vehicle cells. Gln: glutamine, Glu: glutamate, α-KG: alpha-ketoglutarate, Fum: fumarate, Mal: malate, Cit: citrate-isocitrate. Mean ± SEM of triplicates

MDA-MB-453 (968)

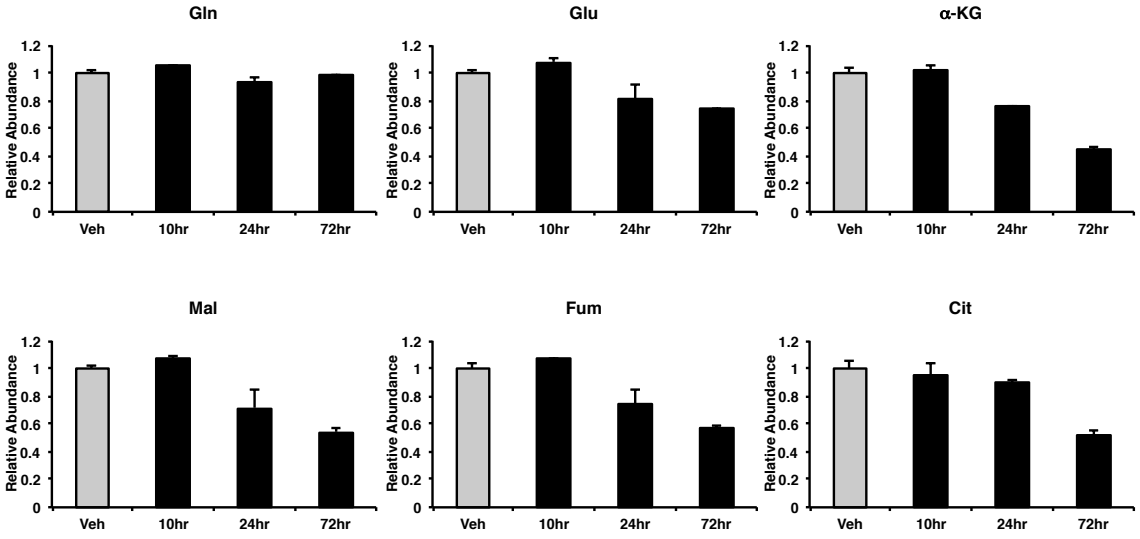

Figure 3.8. 968 requires extended incubation times to inhibit GLS in MDA-MB-231 cells.

Bar graphs depicting relative abundance of relevant TCA cycle intermediates in 968-treated MDA-MB-231 cells compared to the untreated vehicle cells. Gln: glutamine, Glu: glutamate, α-KG: alpha-ketoglutarate, Fum: fumarate, Mal: malate, Cit: citrate-isocitrate. Mean ± SEM of triplicates

MDA-MB-231 (968)

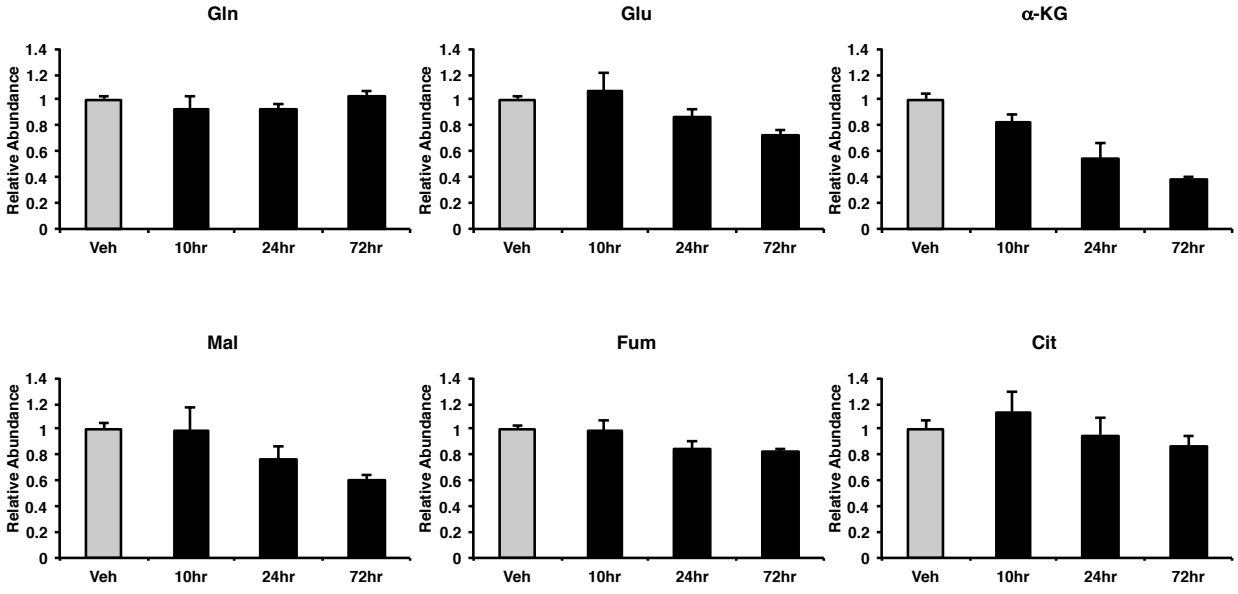

rather than to the catalytically active tetramer species, and it is therefore possible that 968 can only effectively target newly-synthesized glutaminase proteins.

Thus, extended incubation times may allow 968 to bind to newly-synthesized monomers before GLS or GLS2 assemble into their quaternary structure. To this end, we carried out a time-course for 968 treatments on MDA-MB-453 cells (exclusive GLS2 expression) and MDA-MB-231 cells (exclusive GLS expression). This revealed that, over time, 968 treatment increases in potency and effectiveness, leading to decreases in the relative abundances of TCA cycle metabolites downstream of the glutaminase reaction in both luminal and basal breast cancer cell lines (Figure 3.7, Figure 3.8). Together these results show that 968 can indeed inhibit both GLS and GLS2 in monolayer cultured breast cancer cells and that the potency of this inhibition increases with time.

Discussion

Our results reveal that the glutaminase isozyme GLS2 is metabolically active in breast cancer cells. Moreover, basal and luminal breast cancer cells have distinct expression profiles of both GLS and GLS2. Furthermore, both of these enzymes can feed TCA cycle anaplerosis and may be utilized in parallel to varying degrees. These findings have potentially important clinical implications since there is a GLS-specific inhibitor, CB-839, currently in Phase II clinical trials for treatment of breast cancer. Indeed, our findings may help explain the mixed results thus far exhibited by CB-839 in treating breast cancer cells, both *in vivo* and *ex vivo*[7].

The discovery that GLS2 is frequently downregulated in liver cancers, together with early work indicating a pro-oncogenic role for GLS, initially led to the proposal that the two isozymes

play opposing roles during tumorigenesis. However, more recent findings indicate that in certain contexts, GLS2 can be important for tumor progression. For example, a recent loss-of-function screen specifically identified GLS2, but not GLS, as one of the top 16 hits of essential metabolic genes for tumorigenesis[20]. The confusion surrounding the role of GLS2 may have obscured the significance of this finding as it pertains to cancer cell metabolism. One possible explanation for the lack of clarity in the field is that while these homologous enzymes do not have fundamentally different catalytic roles (i.e. they both convert glutamine into glutamate), they are subject to distinct modes of regulation. Indeed, whereas expression of the *GLS* gene is enhanced by oncogenic transcription factors associated with cell-cycle progression [21, 22], transcription of *GLS2* is driven both by the tumor suppressor p53 in response to oxidative stress [12], and also by the proto-oncoprotein N-myc [13]. Disruption of p53 function likely explains some instances of downregulated *GLS2* expression in tumors. However, there are some intrinsic differences between the GLS and GLS2 enzymes that could lead to selective pressure for the former over the latter. In the presence of phosphate, GLS has a significantly higher affinity for glutamine than does GLS2, resulting in a much higher catalytic efficiency[23]. Furthermore, it was recently reported that the distinct GLS2 C-terminus binds to and inhibits the activation of the small GTPase Rac1, resulting in suppressed migration, invasion, and metastasis of liver cancer cell lines [24].

A recent report has found that pancreatic cancer cells can utilize compensatory pathways to combat glutamine inhibition[25]. In this study, the authors treated pancreatic cancers both *in vivo* and *ex vivo* with the glutaminase inhibitor CB-839 and observed a decrease in its ability to affect glutamine metabolism over time. This decrease was linked to the ability of these cancer cells to utilize alternative pathways to synthesize glutamate[25]. In contrast, the 968 treatment

experiments described here had the opposite outcome, increasing in potency over time. Further work is required to determine if the inhibition observed from the 968 treatments will persist at even longer incubation periods. It is tempting to speculate that highly specific inhibitors like CB-839 may prove to be less effective in treating cancers, as the metabolic network of the cell possesses the metabolic plasticity to adapt to this single obstruction to glutamine utilization in cancer cells.

In conclusion, luminal and basal breast cancer cells have distinct expression patterns of the glutaminase isozymes GLS and GLS2. We identify GLS2 as an important metabolically active enzyme in breast cancer, which can supply the TCA cycle in a similar manner to GLS. Finally, we show that 968 requires extended incubation times to improve its efficacy in blocking glutamine-mediated anaplerosis. Identifying GLS2 as an active metabolic enzyme in breast cancers will add yet another layer of complexity to the metabolic heterogeneity of cancer, and may prove to be critical for future improvements in cancer therapies.

Materials and Methods

Cell Culture and Reagents. MCF7, T-47D, MDA-MB-453, MDA-MB-231, TSE and Hs 578T breast cancer cell lines were cultured in full media composed of RPMI 1640, 10% Fetal Bovine Serum (FBS). Cells were cultured in a 37 °C, 5% CO_2 atmosphere. BPTES and 968 (10 uM, final concentration) were added to the media or 0.01% DMSO (cellgro), which represents the vehicle control (Veh). At the start of each experiment, cells were seeded at a density of 2.2×10^6 cells for 10 cm plates for protein collection or 3×10^5 cells/well in a 6-well plate for metabolite collection and allowed to adhere and grow to 80% confluence. Cells were then washed with PBS

and allowed to incubate in the respective treatments for 10 hours. Metabolites were extracted as described below.

Immunoblotting. Whole-cell lysates were prepared in lysis buffer (50 mM HEPES pH 8.0, 150 mM NaCl, 1 mM Na_3VO_4, 25 mM NaF, 1% (v/v) Triton X-100, 1 mM $MgCl_2$, 50 mM β-glycerophosphate, 30 μg ml^{-1} leupeptin, 5 μg ml^{-1} aprotinin) and insoluble debris was pelleted by centrifugation and removed. Protein concentration was determined by Bradford assay (Bio-Rad), and lysate proteins denatured by boiling for 5 min in reducing SDS-sample buffer. Lysate proteins (20 μg total protein/lane) were then resolved on Novex 4–20% Tris-glycine mini or midi protein gels (Life Technologies), and transferred to polyvinylidene difluoride membranes (PerkinElmer). Membranes were blocked in 7% bovine serum albumin in tris-buffered saline and tween 20 (TBST) for 1 h at room temperature, and probed overnight at 4 °C in primary antibody solution in TBST. They were then washed in TBST, and incubated in TBST solution containing 25% (v/v) non-fat dry milk powder and appropriate secondary antibody at the manufacturer's recommended concentration for 1 h. Finally, the membranes were washed in TBST, and bands imaged using Western Lightning Plus-ECL (PerkinElmer) and HyBlot ES autoradiography film (Denville Scientific Inc.).incubated with anti-GLS antibody is Abgent AP8809b at 1:8000, and GLS2 antibody is Abcam ab113509 at 1:5000. The latter recognizes GLS as well, so samples have to be run on a 12% gel to separate the GLS and GLS2 bands.

Metabolite Extraction. The procedures for cultured cells are described in previous studies [26, 27]. Briefly, for adherent cells, the media was quickly aspirated and cells were washed with cold

PBS on dry ice. Then, 1 mL of extraction solvent (80% methanol/water) cooled to -80°C was added immediately to each well, and the dishes were transferred to -80°C for 15 minutes. Plates were removed and cells were scraped into the extraction solvent on dry ice. All metabolite extracts were centrifuged at 20,000g at 4°C for 10 min. Finally, the solvent in each sample was evaporated in a Speed Vacuum for metabolomics analysis. For polar metabolite analysis, the cell extracts were dissolved in 15µL water and 15µL methanol/acetonitrile (1:1 v/v) (LC-MS optima grade, Thermo Scientific). Samples were centrifuged at 20,000g for 10 min at 4°C and the supernatants were transferred to Liquid Chromatography (LC) vials. The injection volume for polar metabolite analysis was 8 uL.

U-^{13}C-Glutamine labeling. Cells were first cultured in standard RPMI 1640, 10% Fetal Bovine Serum (FBS) media to 70% confluence. They were then washed with PBS and treated with the corresponding drug treatments or vehicle in media conditions where glutamine is replaced with U-13-C6-L-glutamine (Cambridge Isotope Laboratories, Inc.) for 10 hours. Metabolites were then extracted as described in the text from the cells and the media.

Liquid Chromatography. An Xbridge amide column (100 x 2.1 mm i.d., 3.5 µm; Waters) was employed on a Dionex (Ultimate 3000 UHPLC) for compound separation at room temperature. The mobile phase A was 20 mM ammonium acetate and 15 mM ammonium hydroxide in water with 3% acetonitrile, pH 9.0, and the mobile phase B was acetonitrile. The linear gradient is as follows: 0 min, 85% B; 1.5 min, 85% B, 5.5 min, 35% B; 10 min, 35% B, 10.5 min, 35% B, 14.5 min, 35% B, 15 min, 85% B, and 20 min, 85% B. The flow rate was 0.15 ml/min from 0 to 10 min and 15 to 20 min, and 0.3 ml/min from 10.5 to 14.5 min. All solvents are LCMS grade and

purchased from Fisher Scientific.

Mass spectrometry. The Q Exactive MS (Thermo Scientific) is equipped with a heated electrospray ionization probe (HESI), and the relevant parameters are as listed: evaporation temperature, 120 °C; sheath gas, 30; auxiliary gas, 10; sweep gas, 3; spray voltage, 3.6 kV for positive mode and 2.5 kV for negative mode. Capillary temperature was set at 320°C, and S-lens was 55. A full scan range from 60 to 900 (m/z) was used. The resolution was set at 70,000. The maximum injection time was 200 ms. Automated gain control (AGC) was targeted at 3,000,000 ions.

Metabolomics and data analysis. Raw data collected from LC-Q Exactive MS was processed on Sieve 2.0 (Thermo Scientific). Peak alignment and detection were performed according to the protocol described by Thermo Scientific. For a targeted metabolite analysis, the method "peak alignment and frame extraction" was applied. An input file of theoretical m/z and detected retention time of 204 known metabolites was used for targeted metabolites analysis with data collected in positive mode, while a separate input file of 278 metabolites was used for negative mode. M/Z width is set at 10 ppm. The output file including detected m/z and relative intensity in different samples is obtained after data processing. Quantitation and statistics were calculated and visualized with Microsoft Excel, MORPHEUS and MetaboAnalyst online software.

GLS and GLS2 Knockdowns

For knockdown of GLS or GLS2, cells were grown in RPMI 1640, 10% FBS media until 70%

confluent, and then transduced with lentiviruses containing MISSION shRNA constructs (Sigma) targeting human GLS or GLS2, or a non-targeting control shRNA construct, in the presence of polybrene, for 48 hours.

References:

1. La Vecchia, C., et al., *Cancer mortality in Europe, 2000-2004, and an overview of trends since 1975.* Ann Oncol, 2010. **21**(6): p. 1323-60.
2. Prat, A. and C.M. Perou, *Deconstructing the molecular portraits of breast cancer.* Mol Oncol, 2011. **5**(1): p. 5-23.
3. Prat, A., et al., *Clinical implications of the intrinsic molecular subtypes of breast cancer.* Breast, 2015. **24 Suppl 2**: p. S26-35.
4. Timmerman, L.A., et al., *Glutamine sensitivity analysis identifies the xCT antiporter as a common triple-negative breast tumor therapeutic target.* Cancer Cell, 2013. **24**(4): p. 450-65.
5. Pavlova, N.N. and C.B. Thompson, *The Emerging Hallmarks of Cancer Metabolism.* Cell Metab, 2016. **23**(1): p. 27-47.
6. Cluntun, A.A., et al., *Glutamine Metabolism in Cancer: Understanding the Heterogeneity.* Trends in Cancer. **3**(3): p. 169-180.
7. Gross, M.I., et al., *Antitumor activity of the glutaminase inhibitor CB-839 in triple-negative breast cancer.* Mol Cancer Ther, 2014. **13**(4): p. 890-901.
8. Katt, W.P. and R.A. Cerione, *Glutaminase regulation in cancer cells: a druggable chain of events.* Drug Discov Today, 2014. **19**(4): p. 450-7.
9. Calvo, S.E., K.R. Clauser, and V.K. Mootha, *MitoCarta2.0: an updated inventory of mammalian mitochondrial proteins.* Nucleic Acids Res, 2016. **44**(D1): p. D1251-7.
10. Altman, B.J., Z.E. Stine, and C.V. Dang, *From Krebs to clinic: glutamine metabolism to cancer therapy.* Nat Rev Cancer, 2016.
11. Hu, W., et al., *Glutaminase 2, a novel p53 target gene regulating energy metabolism and*

antioxidant function. Proc Natl Acad Sci U S A, 2010. **107**(16): p. 7455-60.

12. Suzuki, S., et al., *Phosphate-activated glutaminase (GLS2), a p53-inducible regulator of glutamine metabolism and reactive oxygen species.* Proc Natl Acad Sci U S A, 2010. **107**(16): p. 7461-6.
13. Xiao, D., et al., *Myc promotes glutaminolysis in human neuroblastoma through direct activation of glutaminase 2.* Oncotarget, 2015. **6**(38): p. 40655-66.
14. Giacobbe, A., et al., *p63 regulates glutaminase 2 expression.* Cell Cycle, 2013. **12**(9): p. 1395-405.
15. Xiang, L., et al., *Knock-down of glutaminase 2 expression decreases glutathione, NADH, and sensitizes cervical cancer to ionizing radiation.* Biochim Biophys Acta, 2013. **1833**(12): p. 2996-3005.
16. Robinson, M.M., et al., *Novel mechanism of inhibition of rat kidney-type glutaminase by bis-2-(5-phenylacetamido-1,2,4-thiadiazol-2-yl)ethyl sulfide (BPTES).* Biochem J, 2007. **406**(3): p. 407-14.
17. Stalnecker, C.A., et al., *Mechanism by which a recently discovered allosteric inhibitor blocks glutamine metabolism in transformed cells.* Proc Natl Acad Sci U S A, 2015. **112**(2): p. 394-9.
18. Wang, J.B., et al., *Targeting mitochondrial glutaminase activity inhibits oncogenic transformation.* Cancer Cell, 2010. **18**(3): p. 207-19.
19. Gao, M., et al., *Glutaminolysis and Transferrin Regulate Ferroptosis.* Mol Cell, 2015. **59**(2): p. 298-308.
20. Possemato, R., et al., *Functional genomics reveal that the serine synthesis pathway is essential in breast cancer.* Nature, 2011. **476**(7360): p. 346-50.

21. Gao, P., et al., *c-Myc suppression of miR-23a/b enhances mitochondrial glutaminase expression and glutamine metabolism.* Nature, 2009. **458**(7239): p. 762-5.

22. Lukey, M.J., et al., *The oncogenic transcription factor c-Jun regulates glutaminase expression and sensitizes cells to glutaminase-targeted therapy.* Nat Commun, 2016. **7**: p. 11321.

23. Botman, D., W. Tigchelaar, and C.J. Van Noorden, *Determination of phosphate-activated glutaminase activity and its kinetics in mouse tissues using metabolic mapping (quantitative enzyme histochemistry).* J Histochem Cytochem, 2014. **62**(11): p. 813-26.

24. Zhang, C., et al., *Glutaminase 2 is a novel negative regulator of small GTPase Rac1 and mediates p53 function in suppressing metastasis.* Elife, 2016. **5**: p. e10727.

25. Biancur, D.E., et al., *Compensatory metabolic networks in pancreatic cancers upon perturbation of glutamine metabolism.* Nat Commun, 2017. **8**: p. 15965.

26. Liu, X., et al., *A strategy for sensitive, large scale quantitative metabolomics.* J Vis Exp, 2014(87).

27. Liu, X., Z. Ser, and J.W. Locasale, *Development and quantitative evaluation of a high-resolution metabolomics technology.* Anal Chem, 2014. **86**(4): p. 2175-84.

Chapter 4

Conclusions and future directions

Conclusions

The discovery that glucose was the main source of acetyl groups found on acetylated histones, and that these groups could appear on histone tails within a time period of minutes[1, 2], prompted us to wonder if there was a connection between the increased glycolytic rates observed in cancer cells due to the Warburg effect and histone acetylation patterns. Indeed, the work described in Chapter 2 provides evidence for an unappreciated consequence of the Warburg effect, whereby it carries out signaling functions in cells by altering the levels of multiple key metabolites that serve as cofactors and substrates for reactions involving histone acetylation. Of all metabolites considered in this study, ac-CoA, and the ratio of ac-CoA to CoA, appeared to have the strongest influence on histone acetylation (Figure 2.4.C, D).

Recent work has shown that intracellular ac-CoA levels could manipulate certain acetyltransferases such as p300 and Gcn5[3, 4]. In our study we identified many other residues not known to be catalyzed by these enzymes are also sensitive to the ac-CoA levels, suggesting that such acetylation events are likely pervasive in cells. Additionally, we found that the locations of these modifications on histones seemed to influence their sensitivity to changes in glycolytic flux, thus suggesting that spatial proximity to the metabolic milieu may dictate, in part, histone modifications that are more dynamic. We also identified other histone acylation marks that were sensitive to glycolytic flux, notably, histone butyrylation, histone propionylation and histone 2-hydroxyisobutryrylation (Figure 2.6.). The sensitivity of these posttranslational modifications (PTMs) to glycolytic flux was unexpected and further investigation is required which would benefit from a better understanding of the chemical reaction mechanisms that

mediate these PTMs. Their sensitivity to glycolytic flux may add to the adaptive responses that cancer cells derive from the Warburg effect as glycolytic rates are increased in these cells by as much as 200 fold compared to normal cells. An exciting recent study has demonstrated that resistance to targeted therapy can be driven by elevated nutrient levels[5]. As abnormal metabolism is a recurrent theme in cancer, understanding its effect on chromatin biology may lead to new insights into tumor cell biology and the interactions between metabolism and gene regulation.

Additionally, the 2DG system we developed to manipulate glycolytic flux, beyond being an effective research tool, may have many interesting implications. First, we show that treating cells with low doses of this inhibitor for short time periods can decrease glycolytic flux without completely obstructing it. The implication here is that changes in dose and incubation times may have drastic effects on the effectiveness of therapies targeting metabolic pathways. It is tempting to speculate that this may be an underlying reason for the mixed results obtained with 2DG in cancer therapy[6]. Indeed, recent work on glutaminase inhibitors[7], as well as our studies with 968 described in Chapter 3, supports this notion. Given the strong connections between metabolism and epigenetics[8], I would go as far as to recommend that any drug treatment that targets a metabolic pathway, should also be assessed for its effects on the epigenome, before any conclusions can be made regarding its effectiveness as a therapy.

Glutaminase has long been thought to be an important enzyme for cancer cell survival. However, most of the attention in the field has been given almost exclusively to GLS and not to its isozyme GLS2. Our finding that GLS2 is a metabolically active enzyme that can feed TCA cycle anaplerosis in breast cancer cells in a similar manner to GLS may help change

this trend. With the increasing appreciation of the heterogeneity of glutamine dependency across different cancer types, this finding serves as yet another aspect that may help explain this plasticity. Moreover, we show that luminal and basal breast cancer cells have distinct expression patterns of the glutaminase isozymes GLS and GLS2. As most studies characterizing breast cancers have traditionally been genomic in nature, our findings suggest that the distinct metabolic nature of these subtypes may be in part due to unique isozyme utilization. This point may prove to be critical for treatment, as drugs that inhibit specific isozymes will be ineffective. Following this line of reasoning, we show that the glutaminase allosteric inhibitor 968 can inhibit both GLS and GLS2, but requires longer incubation times than BPTES-like inhibitors to realize its efficacy in blocking glutamine-mediated anaplerosis.

The significance of identifying GLS2 as a metabolically active enzyme cannot be overstated, as many recent studies would have benefitted from this finding. For example, a recent study caused significant confusion and controversy when the authors knocked out GLS in non-small lung carcinomas (NSCLC), both in cell culture and *in vivo*, and saw no deleterious effect on these tumors[9]. Many people took these findings to mean that glutamine metabolism is an artifact of cell culture and that cells grown in live animals do not require it. However, it now appears that these cancer types highly express GLS2 but little if any GLS. Moreover, these cells express pyruvate carboxylase (PC) that can also feed TCA cycle anaplerosis. The fact that none of the reviewers of this paper caught this, or asked the authors to knockdown GLS2, speaks volumes about how the field views the importance of GLS2. Also, pancreatic adenocarcinoma cells (PDACs) are also known to express GLS2[10], yet this was not considered in the design of the recent study that revealed the GLS-specific inhibitor CB-839 lost its efficacy over extended incubation times[7]. Unfortunately, the list of studies that ignore GLS2 is extensive, perhaps in

part because of the conflicting ideas that have been put forward regarding the role of GLS2 in cancer progression. It is my hope that the work described in Chapter 3 of this thesis will help shed new light on how GLS2 contributes to certain types of cancer.

Future directions

The studies presented in this dissertation point to multiple areas worthy of further investigation. From the work presented in Chapter 2, I was able to identify specific histone acylation marks that change in response to glutamine flux. The next logical step would be to perform chromatin immunoprecipitation combined with a massively parallel DNA sequencing (ChIP-seq) experiment on these specific marks to identify those genes that are enriched at these specific marks. To simplify the experiment, I would perform these studies on cells treated with low (0.5 mM) and high (5 mM) concentrations of 2DG, and compare the results with those obtained for the DMSO-treated vehicle. A dynamic change from hyper- to hypo-acylation in response to glycolytic flux localized at specific genes would increase the biological relevance of our study. Furthermore, I would accompany this experiment with an RNA-seq or RT-PCR experiment to confirm that these specific changes in histone acylation marks are affecting the transcription of the underlying genes to which they are localized. This could potentially help develop a useful model whereby cancer cells utilize the Warburg effect to regulate and maintain the expression of specific genes to give these cells a tumorigenic advantage.

It is important to note that some of the histone modifications identified by our study have no known function and it would therefore be very interesting to link any of them to controlling gene expression. Moreover, the link between glycolysis and the corresponding acyl-CoA intermediates that are presumably acting as acyl-donors for the identified histone marks is still

unclear. Although, we assume that this connection may be due the decrease in free CoA, it would be interesting to perform an untargeted metabolomics experiment to identify other less obvious connections that may also exist. It has become increasingly clear that cancer metabolism can be affected by the microenvironment of the cell, thus it would be important to determine if our results persist in the context of 3D-cultured cells and *in vivo* studies.

Lastly, it will also be of interest to extend this study to a panel of cancer and normal cells, that exhibit varying degrees of the Warburg effect (i.e. different rates of glucose consumption) and determine if this is reflected in changes in specific histone acylation marks. Finally, the compartmentalization of cellular metabolism is an important aspect that is often ignored due to the lack of reliable methods to obtain organelle-specific metabolites. However, there have been recent improvements and advances in harvesting mitochondrial metabolites, and it would be interesting to utilize these techniques to determine if the observed changes in ac-CoA levels are happening in the cytosol or the mitochondria. This would be especially interesting when considering the many acyl-CoA intermediates.

The work presented in Chapter 3 serves as a starting point to study GLS2 in cancer. A logical follow up to the ^{13}C-labeling experiment would be to perform a labeled ^{15}N-glutamine tracing experiment on our panel of breast cancer cells. Since both of these enzymes are thought to be catalytically identical, any differences in the observed labeling would be of interest, since there are no studies documenting the two isozymes in this manner. Obviously, extending our studies to cells grown in 3D culture and *in vivo* mouse studies will further our findings and potentially uncover metabolic differences due to changes in the tumor microenvironment. It will be interesting to determine if these different cell growth conditions result in utilizing either of these enzymes preferentially according to changes in the microenvironment of the cells.

Still, another interesting experiment would be to determine where exactly does GLS2 localize within the mitochondria, and if it differs from GLS in this respect. Moreover, it will be important to see where else these isozymes localize in cells. Following up on the 968 results will also be of great importance. Increasing the incubation times can determine if these breast cancer cells ever adapt to these treatments. It will also be interesting to see if 968 behaves in a similar manner when cells are grown in 3D culture or in mice. Finally, extending these studies to determine how active GLS2 is in other cancer types beyond the breast cancer lines used in Chapter 3 will be very important. Lung and pancreatic cancer derived cells would be good subjects of study to determine if GLS2 can explain the observed heterogeneity in glutamine dependency that has been observed in these cells.

References

1. Everts, A.G., et al., *Quantitative dynamics of the link between cellular metabolism and histone acetylation.* J Biol Chem, 2013. **288**(17): p. 12142-51.
2. Zheng, Y., P.M. Thomas, and N.L. Kelleher, *Measurement of acetylation turnover at distinct lysines in human histones identifies long-lived acetylation sites.* Nat Commun, 2013. **4**: p. 2203.
3. Henry, R.A., et al., *Changing the selectivity of p300 by acetyl-CoA modulation of histone acetylation.* ACS Chem Biol, 2015. **10**(1): p. 146-56.
4. Lu, C. and C.B. Thompson, *Metabolic regulation of epigenetics.* Cell Metab, 2012. **16**(1): p. 9-17.
5. Masui, K., et al., *Glucose-dependent acetylation of Rictor promotes targeted cancer therapy resistance.* Proc Natl Acad Sci U S A, 2015.
6. Pelicano, H., et al., *Glycolysis inhibition for anticancer treatment.* Oncogene, 2006. **25**(34): p. 4633-46.
7. Biancur, D.E., et al., *Compensatory metabolic networks in pancreatic cancers upon perturbation of glutamine metabolism.* Nat Commun, 2017. **8**: p. 15965.
8. Kinnaird, A., et al., *Metabolic control of epigenetics in cancer.* Nat Rev Cancer, 2016. **16**(11): p. 694-707.
9. Davidson, S.M., et al., *Environment Impacts the Metabolic Dependencies of Ras-Driven Non-Small Cell Lung Cancer.* Cell Metab, 2016. **23**(3): p. 517-28.
10. Katt, W.P., M.J. Lukey, and R.A. Cerione, *A tale of two glutaminases: homologous enzymes with distinct roles in tumorigenesis.* Future Med Chem, 2017. **9**(2): p. 223-243.

Glossary

Anaplerosis: The process of replenishing metabolic pathway intermediates. For example, carbon that is lost from the TCA cycle to supply biosynthetic reactions can be replenished by glutamine-derived α-KG, glucose-derived oxaloacetate, etc.

Auxotroph: an organism that is unable to synthesize a particular compound required for its growth.

Catabolism: Describes metabolic pathways that breakdown macromolecules into smaller units and release energy. As opposed to Anabolism, which describes energy-consuming biosynthetic metabolic pathways that construct macromolecules to build biomass of the cell.

Epigenetics: The study of heritable changes in gene expression that does not involve changes to the underlying DNA sequence. Often encompassing chemical modifications to the DNA and Histones.

Extracellular Vesicles: Bilayered membrane-enclosed packages that are shed by various cell types including cancer cells and can contain important cargo that facilitates paracrine signaling. These vesicles can be divided into two broad classes according to size and the unique underlying mechanisms of their biogenesis. A large vesicle class with a diameter of 0.2-1 um called microvesicles, which are plasma membrane-derived and result from its budding and fission. And a much smaller class with a diameter of 0.04 to 0.1 um known as exosomes, that are derived from multi-vesicular bodies that reroute and fuse to the plasma membrane for exocytosis[147-149].

***ex vivo*:** taking place outside of a living organism with minimal deviation from natural conditions.

Glutaminolysis: The metabolic breakdown of glutamine.

Immunometabolism: The changes in intracellular metabolic pathways in immune cells that alter their function.

***in vivo*:** taking place in a living organism

Macropinocytosis: A regulated actin-dependent form of endocytosis, which enables the cell to engulf extracellular macromolecules such as proteins.

Warburg Effect: Also known as aerobic glycolysis, is the phenomenon of increased glucose uptake coupled to lactate secretion, regardless of O_2 availability in cancer cells.

Appendix

Complementary Data

Table A.1.1. List of detected histone modifications and their sensitivity to glycolytic flux

Histone Residue	Modification	Domain	Glucose Sensitivity
H3K9	Ac, Bu	Tail	+
H3K14	Ac, Bu	Tail	+
H3K18	Ac, Bu	Tail	+
H3K23	Ac, Pr, Bu	Tail	+
H3K56	Ac	Tail	-
H3K79	Ac	Globular	-
H4K5	Ac, Pr, Bu	Tail	+
H4K8	Ac, Pr, Bu	Tail	+
H4K12	Ac, Pr, Bu	Tail	+
H4K31	Ac	Globular	-
H2AK5	Ac, Bu	Tail	+
H2BK5	Ac, Bu, Hib	Tail	+
H2BK15	Ac, Bu	Tail	+

H2BK16	Ac, Bu	Tail	+
H2BK20	Ac, Bu	Tail	+
H2BK108	Ac	Tail	-